1969

Vapor phase clustering model for water

Richard W. Bolander
Missouri University of Science and Technology

Department: Physics

VAPOR PHASE CLUSTERING MODEL FOR WATER

by

RICHARD WAYNE BOLANDER, 1940

A DISSERTATION

Presented to the Faculty of the Graduate School of the

UNIVERSITY OF MISSOURI - ROLLA

In Partial Fulfillment of the Requirements for the Degree

DOCTOR OF PHILOSOPHY

in

PHYSICS

1969

Advisor

ABSTRACT

Although nucleation phenomena are among the most widespread of all naturally occurring phenomena, even the simplest of nucleation processes, homogeneous nucleation, is poorly understood, particularly the homogeneous nucleation of liquid droplets from water vapor. Homogeneous nucleation involves only molecules of a single substance and does not include the complicating effects due to a substrate or piece of foreign matter. The semiphenomenological liquid drop theories developed nearly three decades ago differ in relatively minor details, with the crucial element of the theory being the derivation of the free energy of formation of the clusters. The clusters are viewed as well-defined incompressible spherical droplets which possess bulk properties. Such considerations do not take into account the details of the transition region at the interface between the two phases. Recent quantum statistical corrections to the theory are merely attempts to formulate a hybrid theory containing both bulk thermodynamic and quantum statistical considerations. This approach fails to relieve the basic inadequacies arising from the use of Gibb's relation in determining the free energy of formation of a very small cluster.

Extensive experimental observations in the Graduate Center for Cloud Physics Research have indicated that the nucleation rate of water droplets from the vapor is nearly

ten times greater in argon than in helium indicating an influence of the noncondensible gas on the clustering.

Furthermore, this laboratory has found that a characteristic heterogeneous component appears to be due to the presence of a few impurity molecules per cubic centimeter; presumably the presence of a single molecule in a cluster may increase the probability of the cluster reaching the critical size by as much as a factor of 10^5. Since the heterogeneous nucleation rate agrees well with the classical Becker-Doring theory, actual homogeneous nucleation of water vapor may well be 10^{-5} below the predictions of the uncorrected classical theory and all the recent quantum statistical correction factors to the theory tend to raise the predicted rate by at least three orders of magnitude. Thus, any agreement between theory and experiment appears to be shattered. Only a molecular theory possesses the capability of dealing properly with the macromolecular properties of clusters, especially clusters containing a few foreign molecules.

In this dissertation, a statistical mechanical technique is developed from which the equilibrium concentrations of clusters of various sizes may be calculated if the bonding structure of the clusters can be predicted and the energy associated with the various structures are known. A clustering model for water in the vapor phase is developed by postulating the maintainance of the tetrahedral coordination of

hydrogen bonding as observed in ice I. The energy states are approximated through the use of estimated stretching and bending force constants for the bonds as obtained from the infrared and Raman spectra of ice I. It is hoped that an extension of this model will enable one to estimate the equilibrium distribution of clusters enabling the determination of the critical nucleus for the homogeneous nucleation rate theory.

The cluster models presented satisfy the conditions that the noncondensible gas is able to participate in the clustering process and an impurity such as hydrogen peroxide is capable of replacing two water molecules in the cluster, replacing a single hydrogen bond with the covalent bond of the peroxide, enabling the theory to consider quasi-homogeneous nucleation processes. Such advances constitute only one step toward handling real nucleation processes such as occur in nature.

ACKNOWLEDGEMENTS

The author gratefully acknowledges the encouragement, advice, and assistance extended by his advisor, Dr. James L. Kassner, Jr., during the course of these studies. Thanks is also due Dr. Joseph T. Zung for his helpful discussions.

Acknowledgement is given to Drs. John B. Hasted and Howard Reiss for their invaluable discussions on the structure of liquid water and the statistical methods applicable to this study.

A special note of appreciation is extended to the staff and the graduate students of the Graduate Center for Cloud Physics Research for their individual help and moral support while this work was in progress.

This research was supported by the Atmospheric Sciences Section of the National Science Foundation, NSF Grant GA-1501.

TABLE OF CONTENTS

ABSTRACT ii

ACKNOWLEDGEMENTS v

TABLE OF CONTENTS vi

LIST OF ILLUSTRATIONS viii

LIST OF TABLES x

INDEX TO SYMBOL DEFINITIONS xi

CHAPTER I, Introduction 1

1. Introductory Remarks 1
2. Historical Background 7
3. Statistical Mechanical Treatments of Small Clusters 12
4. Statement of the Problem 15

CHAPTER II, Structure and Properties of Water 19

1. Structure of Liquid Water 19
2. The Structure of Ice 30
3. The Structure of Water Vapor 34
4. Summary of Concepts to be Utilized in this Study 40

CHAPTER III, Development of Statistical Method and Determination of Hydrogen Bond Energies 41

1. Statistical Thermodynamic Considerations 42
2. Assignment of Internal Energy Levels 48
3. Calculation of Dimer and Trimer Bond Energies . . 54
4. Determination of Dependence of the Binding Energy on the Number of Nearest and Second Nearest Neighbors 60

CHAPTER IV, Vapor Phase Clustering Model 66

1. Description of Model 67
2. Unimolecular Growth of Clusters 74

CHAPTER V, Summary and Discussion 77

1. Summary of Results 77
2. Sources of Errors 79
3. Suggestions for Further Work 84

APPENDIX I, Estimate of Trimer Vibration Frequencies . . 86

APPENDIX II, Estimate of Moments of Inertia 90

APPENDIX III, Estimate of Dipole-Dipole Interaction Energies 93

BIBLIOGRAPHY 96

VITA 101

LIST OF ILLUSTRATIONS

FIGURE		PAGE
1.	Nucleation of Water Droplets from a Helium Atmosphere Saturated with Water Vapor at Four Different Temperatures: 12.5°C, 22.5°C, 32.5°C, and 41.0°C	3
2.	Decrease in Nucleation Rate with Increasing Sensitive Time for an Initial Pre-expansion Temperature of 12.5°C	4
3.	Nucleation of Water Droplets from a System of Argon or Helium Saturated with Water Vapor at 22.5°C	5
4.	Free Energy of Formation, $\Delta G^{o}(r)$ of a Cluster of Radius r	10
5.	The Tetrahedral Coordination of Hydrogen Bonding as Observed in Ice I	20
6.	Five-Molecule Cluster Proposed by Walrafen to Explain the Infrared and Raman Spectra of Liquid Water.	23
7.	The Structure of Gas Hydrates Containing a Hydrogen Bonded Framework of 46 Water Molecules.	25
8.	Water Molecules in Ice Crystal	31
9.	The Internal Coordinates of the Water Trimer and Dimer	51
10.	The Three Possible Orientations for the Water Molecules in the Trimer	56
11.	Nearest Neighbor Binding Energy, E_b, and the Second Nearest Neighbor Binding Energy, E'	64
12.	Side View of Pentagonal Dodecahedron	70
13.	Top View of Pentagonal Dodecahedron	70
14.	Dodecahedral Cluster of Twenty Water Molecules	71

FIGURE PAGE

15. Dodecahedral Cluster of Water Molecules with Smaller Radii for the Atoms to Show the Structure 71

16. Water Clusters Containing Four, Five, Six, Seven, Eight, and Nine Molecules 74

17. Water Clusters Containing Ten and Eleven Molecules 75

18. Water Clusters Containing Seventeen, Fifty-seven, and Seventy Molecules 76

LIST OF TABLES

TABLE		PAGE
I.	Temperature Dependence of Dielectric Constant, ϵ, with Observed and Calculated Values . . .	21
II.	The Coefficients of the Pressure Series for the Equation of State of Water Vapor as Reported by Keyes.	38
III.	The Values of the Second, Third, and Fourth Equilibrium Constants as Determined from the Equation of State of Keys	39
IV.	Variation of the (O-H) Stretching Frequencies with the Hydrogen Bond Length in Various Hydroxides	55
V.	Parameters used in the Calculation of the Dimer and Trimer Potential Energies . . .	56
VI.	Cluster Binding Energies for the Water Dimer in the Vapor Phase, E_2^o, (kcal/mole) .	58
VII.	Dimer Binding Energy as Calculated by Various Authors	59
VIII.	Trimer Binding Energies, E_3^o, Calculated Using the Parameters Listed in Table V. The Hydrogen Bond Length, R(O-H...O), is Assumed to be 2.90 Å	61
IX.	Dimer and Trimer Binding Energies Exclusive of the Dipole-Dipole Contributions	63

INDEX TO SYMBOL DEFINITIONS

SYMBOL	PAGE	SYMBOL	PAGE
α	62	k_θ	49
A_g	45	N	35
β	62	N_g	35
B_g	45	n	36
Γ_g	45	n_g	36
C_g	45	Q	44
E_g^o	44	Q_g	44
$E_{g\dot{m}}^n$	45	Q_{ge}	44
E_h	62	Q_{gi}	44
E'	62	Q_{gr}	44
f_{gm}	45	Q_{gt}	44
g	35	q_g	46
$I_{g\dot{m}}$	46	R	53
K_g	35	σ	9
k_r	49	σ_g	45
		X_s	45

CHAPTER I

INTRODUCTION

I-1. Introductory Remarks. Scientists have long been involved in the study of the formation and growth of liquid droplets from the vapor phase.[1] The physics of droplet formation is concerned with a number of nucleation processes, most of which may be identified as heterogeneous nucleation, in which the droplet is formed on a fragment of particulate matter which is present in the system. This study is concerned with homogeneous nucleation, nucleation in a system with no impurities present, and quasi-homogeneous nucleation in which only a few foreign molecules participate in the clustering process in addition to molecules of the parent phase.

Various workers at the Graduate Center for Cloud Physics Research, University of Missouri - Rolla, have developed expansion cloud chamber technique to such an extent that more experimental detail is now available concerning the nucleation of liquid droplets from very pure water vapor. Allen[2] has noted the appearance of two distinct aspects of the nucleation process. The first he identifies as a form of heterogeneous nucleation which occurs on a neutral center (presumably individual molecules of some reactive substance) and is superimposed on the homogeneous nucleation process. Since this type of nucleation is closely related to the homogeneous nucleation process, i.e., no particulate matter is involved,

it is proposed to refer to this as quasi-homogeneous nucleation.

The results of Allen's work are reproduced in Figure 1. It was expected that for a given starting temperature, the total nucleation occurring for a given sensitive time should increase more or less exponentially with increasing peak supersaturation. However, the increase in number of droplets formed with increasing supersaturation appears to indicate two separate nucleation processes. The initial type of nucleation cannot be sustained in time if a limited number of centers are initially present; the nucleation rate would decay out with increasing time. This assumption is borne out in Allen's experiments where the nucleation was measured as a function of increasing sensitive time, Figure 2. At higher supersaturations the effect of the initial quasi-homogeneous form of nucleation is apparently swamped by homogeneous nucleation. In between there is a transition region. In Figure 3, it can be seen that the nucleation rate agrees closely with the predictions of the Becker-Doring theory at only one point which lies well within the region of the quasi-homogeneous form of nucleation. If this interpretation is correct, the actual homogeneous nucleation rate for liquid water droplets from the vapor is at least 10^4 to 10^5 smaller than that predicted by the classical theory. Allen suggested that the presence of a neutral molecular

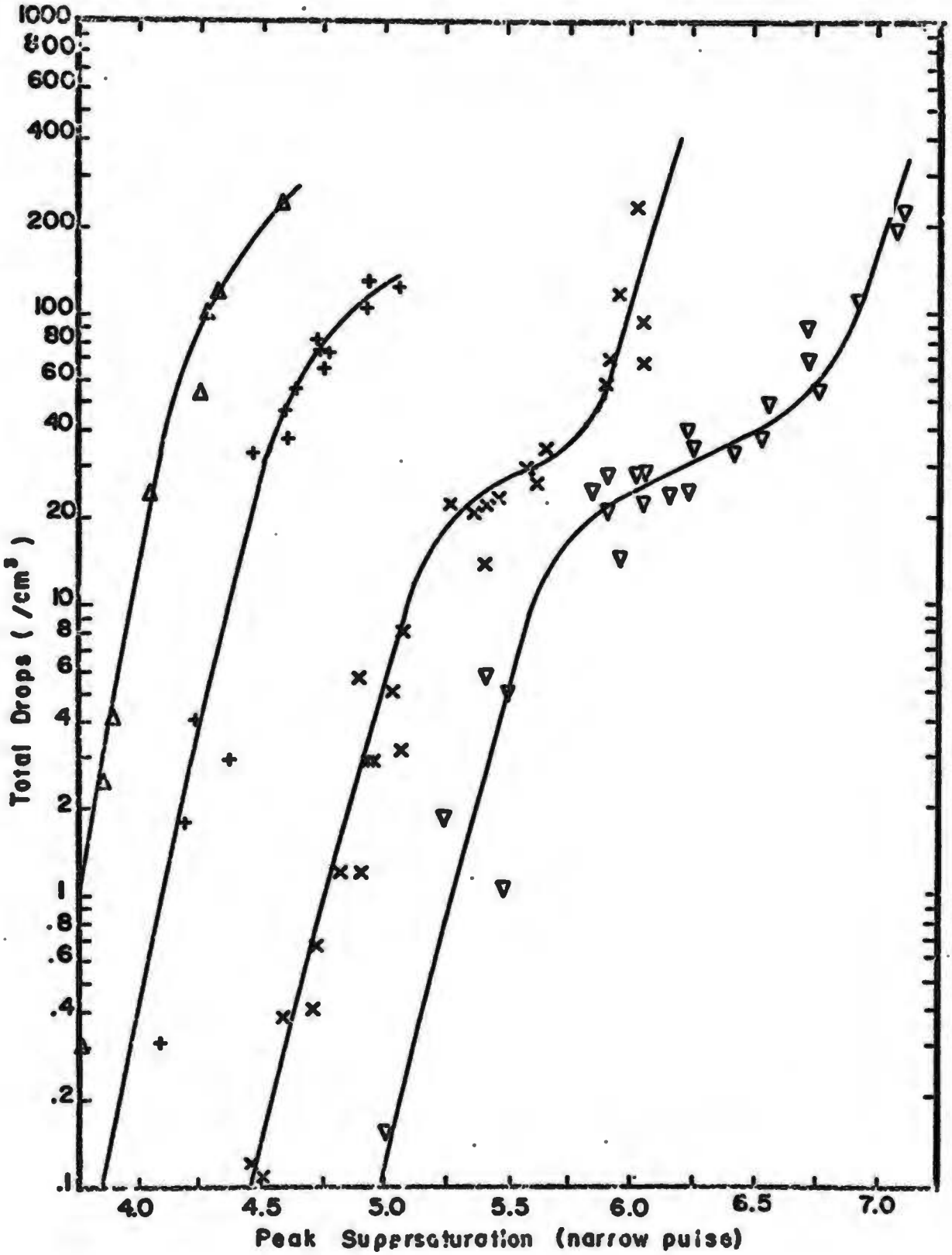

Figure 1. Nucleation of Water Droplets from a Helium Atmosphere Saturated with Water Vapor at Four Different Temperatures: ▽ 12.5°C, X 22.5°C, + 32.5°C, and Δ 41.0°C.

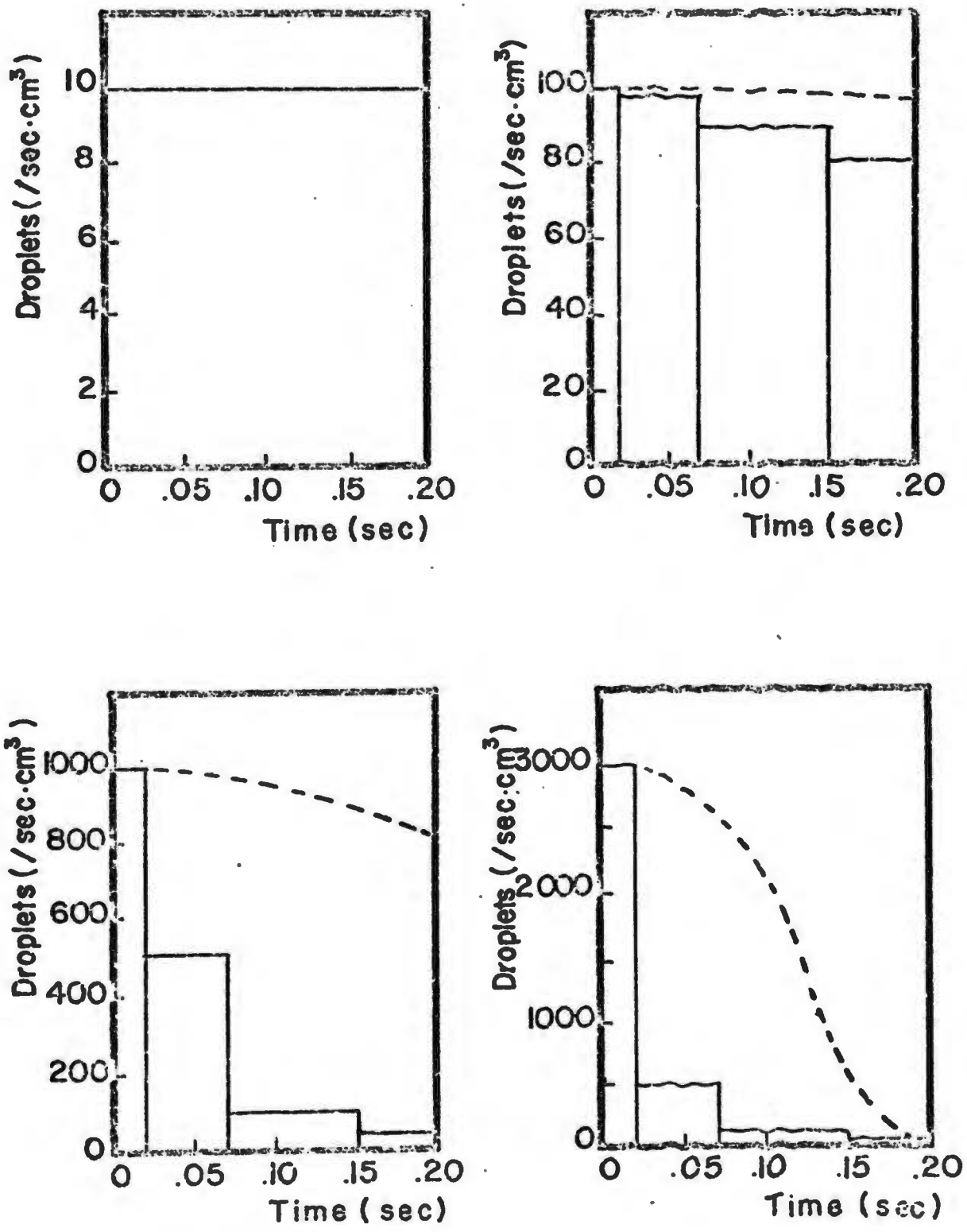

Figure 2. Decrease in Nucleation Rate with Increasing Sensitive Time for an Initial Pre-expansion Temperature of 12.5°C.

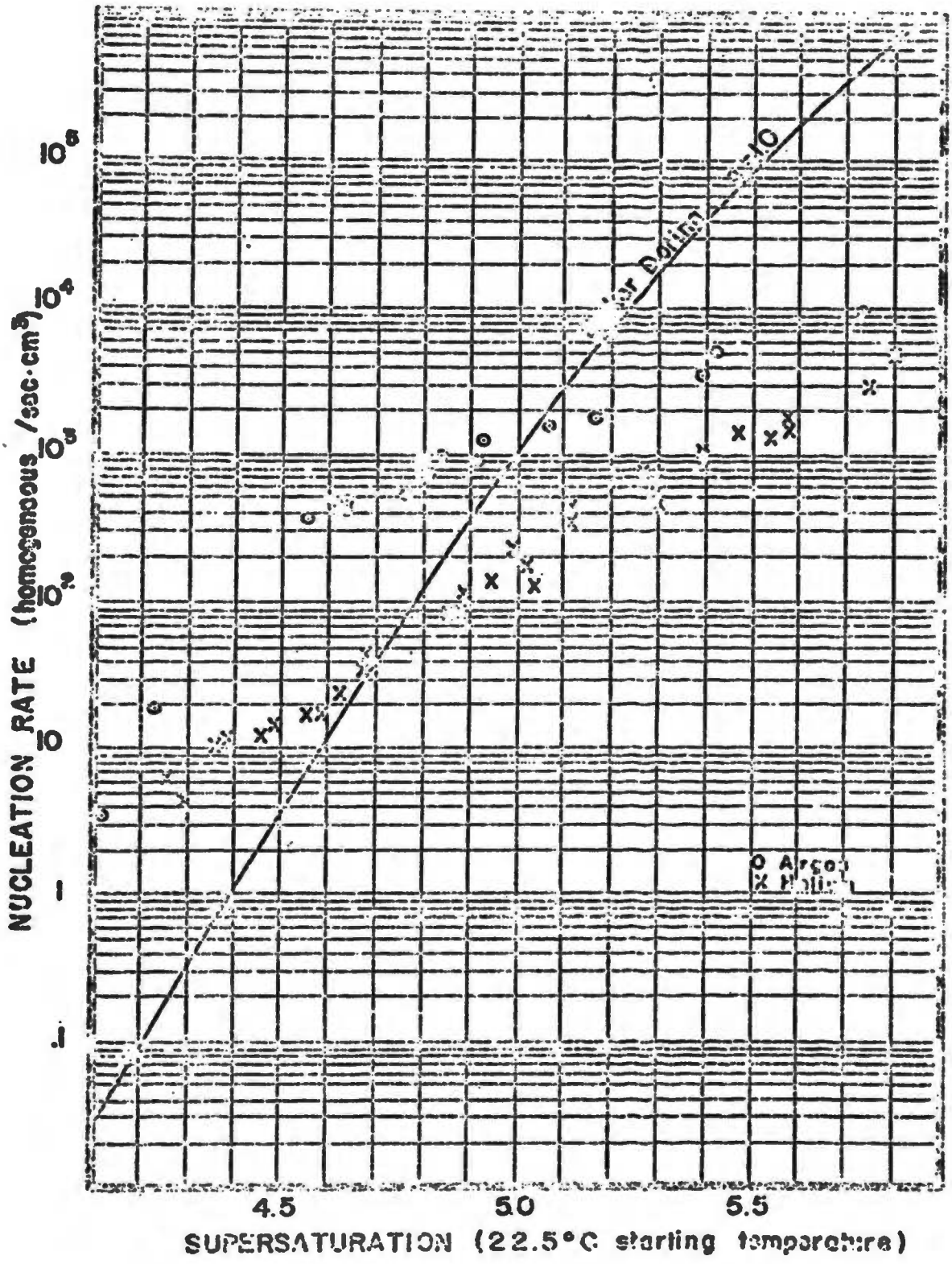

Figure 3. Nucleation of Water Droplets from a System of Argon or Helium Saturated with Water Vapor at 22.5°C.

nucleating center such as hydrogen peroxide may be capable of participating in the clustering process through hydrogen bonding.

Allen also observed a definite effect due to the non-condensible gas used in the cloud chamber as indicated in Figure 3. These observations indicate a probable hydration of the non-condensible gas in the structure of the clusters. Parungo and Lodge[3] have reported a definite influence of helium and argon on the freezing point of supercooled water. Thus, the nucleation of water vapor is much more complex than has been previously supposed.

The problem presented here is to develop a model for the clustering of water molecules in the vapor phase which has the potential for explaining the nucleation data from the cloud chamber experiments such as those mentioned above. The clustering model should be compatible with the liquid and solid structures and with various physical properties such as surface tension, capillary behaviour, and transport properties. The model must be consistent with allied theories for the properties of water in all three phases if it is to be of any practical value in understanding the nucleation process from a molecular point of view. Moreover, it is hoped that this work will provide further insight into the structure of liquid water.

I-2. Historical Background. Before 1875, there was general agreement among scientists that foreign particles must be present before condensation could occur. The concept of homogeneous (or spontaneous) nucleation was not an acceptable explanation. C. T. R. Wilson[4] demonstrated experimentally that homogeneous nucleation existed and that it was definitely distinct from heterogeneous nucleation. Gibbs[5] pointed out the importance of the idea of the work of formation of a drop of a new phase within a parent phase. The work of formation is now commonly called the free energy of formation. Volmer and Weber,[6] following Boltzmann's statistics associated the number of nuclei present in a system with the exponential function of the work of formation, and Farkas[7] laid the foundations for the kinetics of nucleation. These ideas were further developed by Volmer,[8] Kaischew and Stranski,[9] and Becker and Doring[10]; the latter gave the first kinetic formula which contained no unknown constant, and which agreed particularly well with experimental observation. In 1939, Volmer[11] published his important work Kinetik der Phasenbildung and Frenkel[12] perfected the thermodynamics of embryos, while the thesis of Bijl[13] developed similar ideas.

Several reviews of the classical theory of nucleation have been written and the general agreement is that much work remains to be done in this area.[14-22] All of the present nucleation theory which is in a form suitable for quantitive

comparison with experimental data contains the assumption that macroscopic thermodynamic quantities may be assigned to clusters containing only a few molecules. Such treatments have been characterized as semiphenomenological in contrast to a truly molecular approach. Various workers[20,23-27] have included the free energy of translation and rotation of the free gasified cluster and concluded that theoretical nucleation rates were about 10^{18} times faster than predicted by the classical theory. Other workers[28,29] also included cluster translation and rotation but concluded that the correction factor was only about 10^{4}. Courtney[22] demonstrates that monomer loss to the clusters introduces a significant error in the simplifying assumption of the classical theory that the change in the monomer concentration is negligible. As indicated in the preceding discussion, the classical theory fails to give satisfactory agreement with the details of the experiment so that one might expect that more is involved than a simple factor of 10^{18} or 10^{4} as the case may be.

Steady state theories as developed by Volmer,[8] Weber,[6] and Becker and Doring[10] treat the growth of clusters from a supersaturated vapor of monomers by a series of bimolecular reactions in which the clusters grow by the addition of a single molecule per reaction. Growth through collisions between clusters is considered highly improbable because of the low relative concentration of clusters as compared to

monomers. The clusters develop initially with an increase in free energy until a critical size is attained, after which further growth results in a decrease in free energy. The nucleation rate is evaluated by introducing the mathematical artifice of breaking down the clusters larger than the critical size and returning them to the monomer state.

Subject to the assumption that macroscopic properties may be applied to the clusters, the surface and volume contributions to the free energy of formation[10] are shown to be

$$\Delta G^{o}(r) = 4\pi r^{2}\sigma - (4\pi r^{3}kT/3v_{m})\ln S$$

where r is the radius of a spherical embryo; σ is the specific interfacial free energy; v_m, molecular volume in the liquid; and $S = p/p_\infty$, the supersaturation. The actual vapor pressure is represented by p while p_∞ is the vapor pressure over the bulk liquid at equilibrium. Figure 4 shows the behavior of $\Delta G^{o}(r)$ as a function of droplet radius. Clusters smaller than the critical radius, r*, are referred to as embryos while larger droplets are termed nuclei of the liquid phase. Embryos tend to break up into smaller units while nuclei tend to grow.

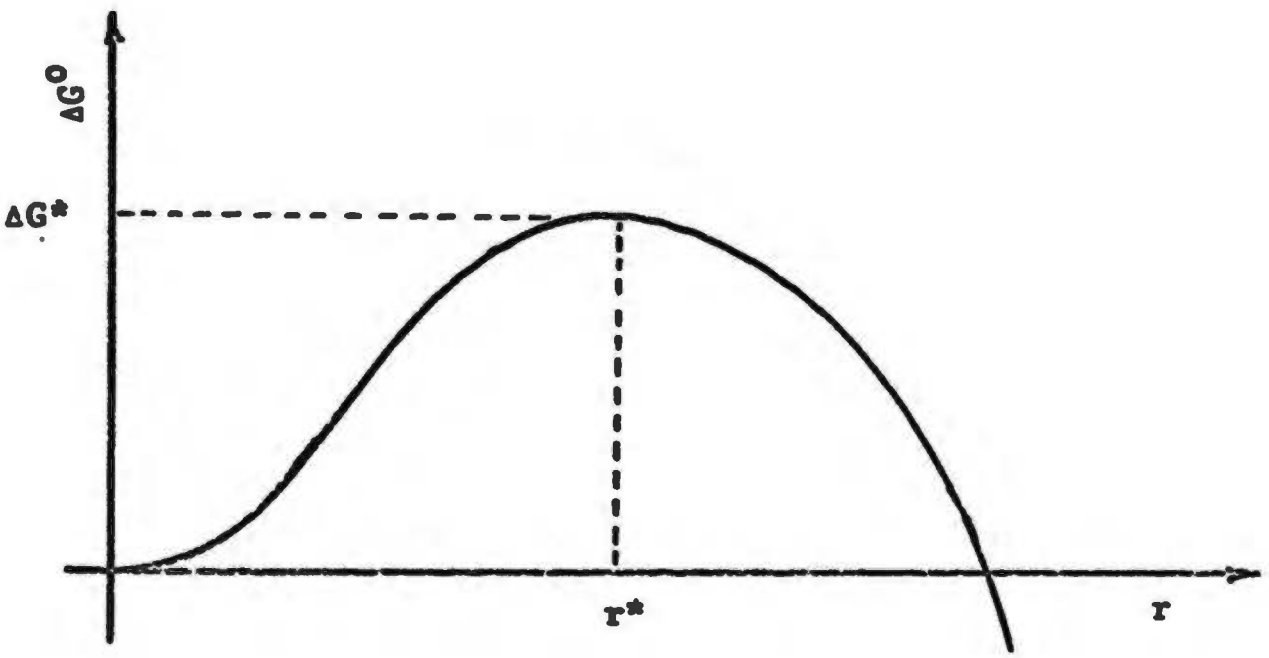

Figure 4. Free Energy of Formation, $_{\Delta}G^{o}(r)$ of a Cluster of Radius r.

The critical radius and free energy of formation of the critical cluster are found to be

$$r^* = (2\sigma v_m)/(kT \ln S)$$

$$\Delta G^* = (16\pi\sigma^3 v_m^2)/(3k^2T^2 \ln^2 S)$$

$$g^* = (32\pi\sigma^3 v_m^2)/(3k^3T^3 \ln S)$$

where g^* is the number of molecules in the critical cluster. These results were first obtained by Gibbs[5] who limited their application to large drops only. Their use for clusters containing 100 molecules or less is questionable, especially due to the use of bulk properties in the evaluation of the

free energy of formation of the clusters. The size of the critical cluster decreases with increasing supersaturation so that the use of the bulk values becomes even more questionable at the higher supersaturations associated with large nucleation rates.

Frenkel[12] and Bijl[13] applied the law of mass action (expressed in mole fractions) in order to determine the equilibrium concentrations of the various cluster sizes,

$$x_g = x_1^g \exp(-\Delta G_g^o/kT) ,$$

where

$$x_g = n_g / \sum_g n_g ,$$

and obtained a Boltzmann-type concentration distribution,

$$n_g = n_1 \exp(-\Delta G_g^o/kT) .$$

This is the expression that has been involved in much of the controversy mentioned on the previous pages. The basic question is how to properly evaluate ΔG_g^o.

Volmer and Weber[6] established the nucleation rate, J, in terms of the rate of collision of a critical nucleus with the monomers, i.e.,

$$J = 4\pi r^{*2} \omega n_{g^*}$$

where ω, the collision frequency, may be determined from kinetic theory. The resulting expression is

$$J = \alpha_c (4\pi r^{*2}) [p/(2\pi mkT)^{1/2}] (p/kT) \exp(-\Delta G^{o}_{g*}/kT)$$

where m represents the mass of a single water molecule. The probability that a collision results in growth (sticking coefficient) is expressed by the factor α_c. Becker and Doring[10] and Zeldovich[30] refined the treatment by considering a steady-state cluster distribution and determining the unimolecular reactions for rate of growth of the clusters and obtained the relationship

$$J = \alpha_c (p/\rho kT)(2\sigma m/\pi)^{1/2} n_{g*}$$

in which ρ is the liquid density and σ is the specific interfacial free energy. This is the nucleation rate exhibited in Figure 3 as the Becker-Doring theory.

I-3. Statistical Mechanical Treatments of Small Clusters. More recent work has developed statistical mechanical treatments of the thermodynamics of small clusters of monatomic molecules with no internal structure.[31-39] These methods are of importance in the present work; however, several typical assumptions are not of use to us because of the ordering introduced by the presence of the hydrogen bonding in clusters of water molecules.

The cell model, developed by Reiss,[36] reduces to the computation of the multiple occupation, by molecules, of cells. This is accomplished by the evaluation of the configuration

integral for a supersaturated assembly. The first fragments of the stable phase are not considered to be spherical liquid droplets. The volume V containing the gas is divided into cubical cells each having the volume

$$\tau = nV/N$$

where n is a positive number greater or less than unity and N is the total number of molecules in the system. The configuration integral is then expressed as a sum of terms of the type

$$\exp(-W/kT)\ (d\omega)^N$$

where W is the configurational potential energy and $d\omega$ stands for the translational volume element of a single molecule in configuration space. The series of terms belonging to a single picture, (a particular specification of the number of molecules in each cell), are generated by arranging the molecules differently within their cells or by permuting the N molecules among the various cells without changing the number in each cell. It is shown that the distribution n(g), the number of cells containing g molecules, is given by

$$n(g) = (N/n)\ \exp\{-[kT(n - g + g\ \ln[g/n]) + \langle\omega(g)\rangle_{Av}]/kT\}$$

where $\langle\omega(g)\rangle_{Av}$ is the average mutual-intercell energy per

g-cell averaged over the environments of all the g-cells in the configuration picture. The main problem in this approach is the evaluation of $\langle\omega(g)\rangle_{Av}$. These calculations are fairly successful for molecules which are nonpolar and have molecular interactions which are chiefly of the dispersion type. The first step is to assume that the average distribution of matter in a g-cell is uniform and that the cell is surrounded by gas of density N/V. These assumptions are not valid when one is concerned with hydrogen bonded, polar molecules which form highly structured clusters.[87]

Another approach is to treat the gas as a mixture of physical clusters containing various numbers of molecules.[20] The standard procedure in this approach is to assume the clusters of molecules are bound together by their van der Waals attractions and the mechanism of cluster formation is due to elastic collision processes.[74] The resulting distribution n_g of g-clusters is

$$n_g = Q_g(n_1/Q_1)^g$$

where Q_g is the independent cluster partition function of a g-cluster. The problem is to determine the values of the various Q_g's. An approximation which appears to give satisfactory results for monoatomic, non-polar gases is to assume that the total vibrational energy of clusters is distributed uniformly among the various internal degrees of

freedom so that the mean g-cluster vibrational energy, $\bar{\varepsilon}$, is

$$\bar{\varepsilon} = X_g kT$$

where X_g represents the number of internal degrees of freedom of a g-cluster. This assumption would be expected to break down if the cluster has interactions present which are as strong as the hydrogen bond. Considering the simple harmonic average energy expression measured with respect to the ground state vibrational level,[74]

$$\bar{\varepsilon}_i = k\theta_i (\exp(\theta_i/T) - 1)^{-1} \quad ,$$

where $\theta_i = h\nu_i/k$ is the characteristic temperature of the oscillator, the average energy is ≈ 0.9 kT when $T = 5\,\theta$, so the assumption is valid only if $T>5\theta$. Characteristic temperatures for stretching and bending hydrogen bonds are of the order of 100-400°K, so the internal modes cannot be assumed to be completely activated. This requires a detailed knowledge of the cluster structure and the characteristic cluster vibration frequencies.

I-4. Statement of the Problem. The general statistical mechanical treatments of clustering in an imperfect gas lead to configuration integrals which cannot be readily evaluated except in a few simple cases. Therefore, little headway can be made toward evaluating nucleation rates for

real vapors. Moreover, the usual cell model procedures for calculating the cluster energy neglect cell structure and assume that all the internal degrees of freedom are excited.

The structural coordination provided by hydrogen bonding, in the case of water molecules, is assumed to provide the simplification needed to make headway in a proper statistical mechanical treatment of gas phase clustering in water vapor. It is assumed that clustering proceeds in such a manner that maximum symmetry is maintained and only the most stable configurations of a given cluster size need be considered.

Physical models for the clusters are built maintaining closely the tetrahedral coordination afforded by hydrogen bonding. It would appear from these models that the vapor phase clusters bear very little resemblance of the structure found in bulk water. By evaluating the binding energy of the cluster and by determining the average internal excitation energy for each cluster under conditions such that the cluster is in thermal equilibrium with the surroundings, it is possible to evaluate the free energy of formation for each cluster species and thereby determine its probability of formation. Such calculations require a knowledge of the energy of interaction between hydrogen bonded molecules and information about the effective force constants for the various modes of vibration. In the absence of reliable theoretical information, it is necessary to resort to semiempirical

determination of these parameters.

An attempt is made to establish a set of empirical parameters describing the interaction of water molecules in various states of hydrogen bonding which can be applied in a consistent fashion to the theoretical description of water in all three phases. The vibration frequencies and libration (torsion) frequencies of the hydrogen bonded species are estimated from infrared and Raman spectra and energy level assignments are made from an empirical determination of the hydrogen bond energy in the water dimer and trimer, utilizing a virial equation of state for water vapor and a standard statistical mechanical theory of clustering. With this information available, it is possible to extend the statistical mechanical treatment to large clusters, determining their free energy of formation and their equilibrium concentration provided the very complex vibrational motions of large clusters can be determined, see Figures 16 through 18. The low frequency vibrations which possess characteristic temperatures in the range of interest contribute most strongly to the partition function. In these cases it may be most convenient to determine these frequencies by experiment with physical models where the spring constants bear a definite relation to the molecular species.

In determining the free energy of formation of a cluster there are two primary contributions (1) the negative binding energy and (2) the positive equilibrium excitation energy.

In general the magnitude of the equilibrium excitation energy exceeds the binding energy slightly so that the free energy of formation is slightly positive as depicted by the classical theory in Figure 4. However, as depicted in Figure 16, the completed ring structures might be expected to be particularly stable because they maximize the number of bonds which increases the binding energy and stiffens the framework so that the characteristic temperatures of the vibration and libration motions are increased. Thus, the statistical mechanical results would not provide a smooth curve for the free energy of formation as is the case of classical theory, see Figure 4. In the case of nucleation, the determination of the characteristics of the critical cluster are all important since it determines the nucleation rate.

Unfortunately, it has not been possible to carry this ambitious project to completion. The work reported in this dissertation comprises the determination of the empirical form of the cluster interaction potential energy and the development of the clustering model for water molecules in the vapor phase.

CHAPTER II

STRUCTURE AND PROPERTIES OF WATER

In order to develop a clustering model for water in the vapor phase, a complete understanding of the structure and behaviour of water in the vapor, liquid, and solid phases is necessary. The vapor clustering model must be compatible with the liquid and solid structures if it is to be valid. The purpose of this chapter is to present the known characteristics of water in the three phases. This information is then utilized in the calculation of the cluster binding energies in Chapter III.

II-1. Structure of Liquid Water. Liquid water possesses several unique properties indicating a basic difference between water and most other liquids. Included are the high melting and boiling points, high heat capacity, increase in density upon melting, and the ability to supercool. These properties indicate extraordinary intermolecular interactions leading to strong association of molecules within the liquid phase. A review of theories prior to 1927 is presented by Chadwell.[40] The generally accepted explanation of this strong association is that hydrogen bonding provides the interaction. An excellent review of the current concepts of hydrogen bonding is presented by Pimentel and McClellan.[41] There are two distinct schools of thought concerning the structure;[42] one

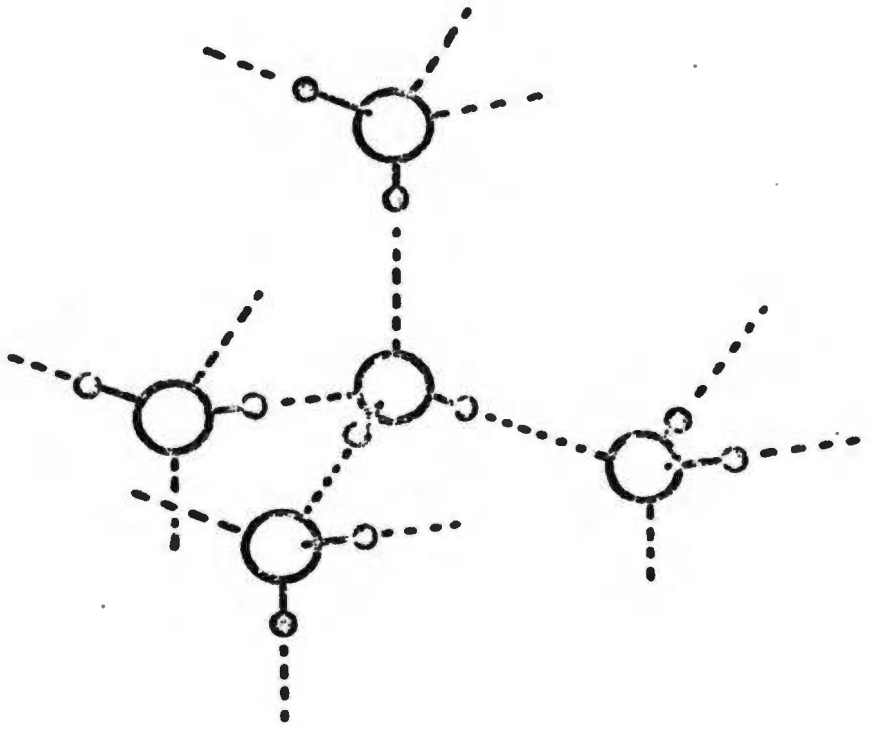

Figure 5. The Tetrahedral Coordination of Hydrogen Bonding as Observed in Ice I.

being the continuum model which best fits the infrared spectrum of the liquid,[42] and the cluster mixture model. The continuum model suggests a gradual weakening of hydrogen bonds by stretching and bending, while the cluster mixture model supports an increased number of broken bonds with increasing temperature posing the problem that one must define when a bond is broken.

The water molecule can participate in four hydrogen bonds, two of them involving the two hydrogens of the molecule and two the lone pairs of electrons of the oxygen with the hydrogens of two neighboring molecules as shown in Figure 5. This tetrahedral coordination is consistent with X-ray diffraction

studies and has been assumed by most workers in liquid water. Oster and Kirkwood[43] used the tetrahedrally hydrogen bonded model for water and assumed free rotation about rigid, directed hydrogen bonds. Pople[44] postulated bendable hydrogen bonds that could rotate and calculated the effect of the first three shells of nearest neighbors. Harris and Alder[45] refined Pople's model to account for polarization resulting from the distortion of the molecules in a field and obtained excellent agreement with the observed temperature dependence for the dielectric constant. Haggis, Hasted, and Buchanan[46] incorporated a model allowing for some molecules to have no hydrogen bonds, some having one hydrogen bond, others two, three and four. In other respects, their model was similar to that of Oster and Kirkwood. This model was also successful in predicting the behaviour of the dielectric constant.

TABLE I

Temperature Dependence of Dielectric Constant, ε, with observed and calculated Values.

T	43*	44*	45*	46*	obs.
0°C	84.2	71.9	90.7	89.0	88.0
25	78.2	63.8	79.9	78.3	78.5
62	72.5	53.0	65.7	--	66.1
83	67.5	47.8	59.6	--	59.9

*references.

The model used by Haggis and co-workers is the same as that utilized by Nemethy and Scheraga[47] and Eadie[95] in their work. They obtained excellent agreement with the experimental values of free energy, enthalpy, and entropy, but the deviation from the specific heat at constant pressure is not acceptable. Nemethy and Scheraga determined the thermodynamic parameters of liquid water by means of a simplified statistical thermodynamic treatment, based on the "flickering cluster" model developed by Frank and Wen.[48] This model is satisfactory in accounting qualitatively for quantities such as density, relaxation times, structural changes in solutions of nonpolar substances, and the accompanying changes in the thermodynamic parameters.

The X-ray diffraction studies of liquid water indicate an increase in the number of nearest neighbors over that observed in ice.[49,50] The distance between nearest neighbors increases from 2.90 Å. at 1.5 °C to 3.05 Å. at 83 °C. The standard explanation is that in water the tetrahedral structure is partially broken down with near neighbors at a variety of distances. This effectively increases the number of near neighbors, and the increase in density due to the "filling in" effect compensates for the decrease in density due to the larger intermolecular distance. As the temperature is increased above 0 °C, two opposing effects occur. The breaking down of the tetrahedral structure

allows more neighboring molecules, thus increasing the density. The increase in molecular distance tends to decrease the density, so that at 4 °C the maximum density of water is the result of these two opposing effects.

This concept of the "broken down ice structure" is certainly very descriptive of the characteristics of liquid water, and is basicaly the concept adopted by Nemethy and Scheraga in their work. Cross, Burnham, and Leighton[51] concluded from Raman spectra that the liquid contains considerable amounts of molecules with four, three, and two hydrogen bonds. Walrafen[52] related the Raman frequencies, polarizations, and infrared frequencies to a five-molecule hydrogen-bonded model indicated in Figure 6 .

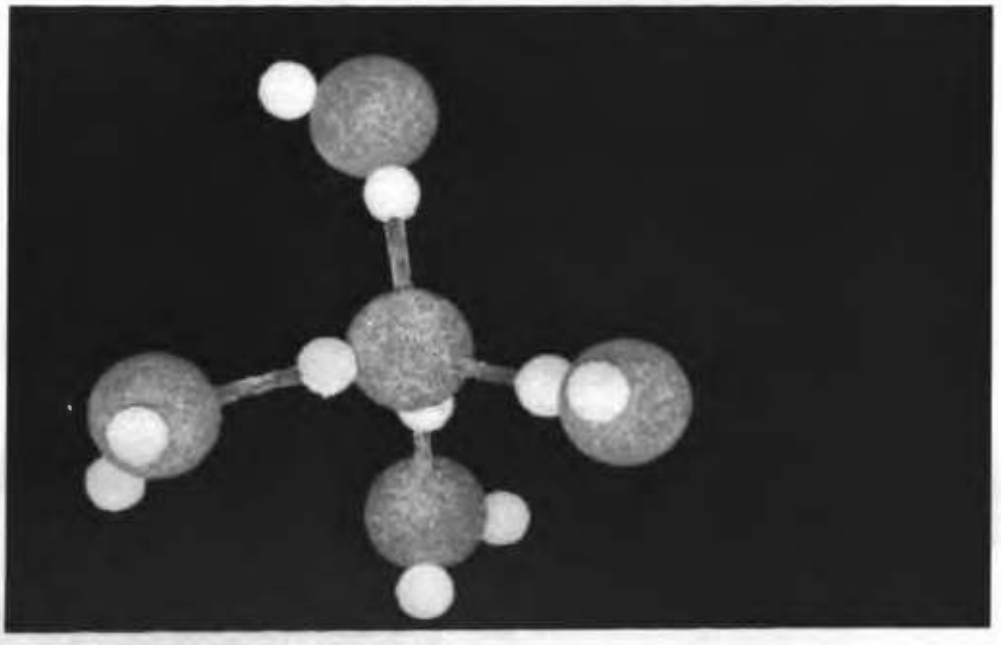

Figure 6. Five-molecule Cluster proposed by Walrafen[52] to explain the Infrared and Raman Spectra of Liquid Water.

Pauling[53,54] has suggested a model for liquid water which is similar in structure to the clathrate structure found in a large number of crystalline hydrates. Typical hydrates are $Cl_2 \cdot 8H_2O$, $Kr \cdot 6H_2O$, $CH_4 \cdot 6H_2O$, and $CHCl_3 \cdot 18H_2O$. X-ray investigation by von Stackelberg[55,56] has indicated cubic structures with edges of the unit cells being 17 Å and 12 Å. The unit cell of these structures was developed by Claussen[57] and they consist of pentagonal dodecahedra, hydrogen bonded in a three dimensional framework. Pauling's model for liquid water is based on the 12 Å clathrate structure. It consists of pentagonal dodecahedra which form eight hydrogen bonds with eight surrounding dodecahedra. There are six water molecules in positions (½,¼,0), etc., each of which forms four hydrogen bonds with molecules of the four surrounding dodecahedra in such a way that a complete framework of 46 water molecules per unit cube is achieved. This structure is shown in Figure 7.

There are two types of cavities; there are two positions at the centers of the dodecahedra, in which molecules with van der Waals' diameter not over 5 Å may be placed, and there are six positions where molecules not larger than 6 Å may be found. Pauling suggests that water may have a structure based on a complex of 21 molecules, 20 of which lie at the corners of a dodecahedron, each molecule forming three

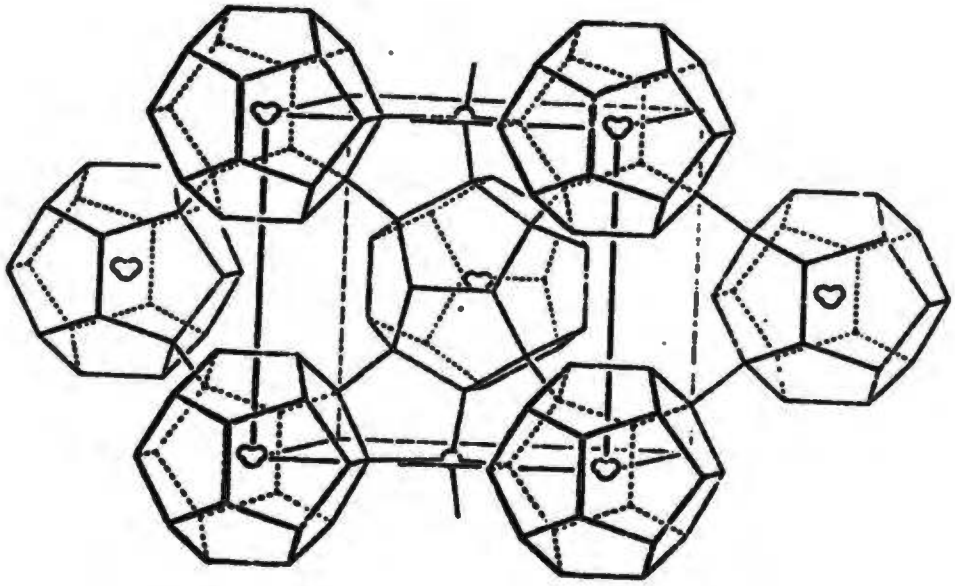

Figure 7. The Structure of Gas Hydrates Containing a Hydrogen Bonded Framework of 46 Water Molecules (from Pauling, reference 53).

hydrogen bonds with the adjacent neighbors in the dodecahedron, and the 21st forming no hydrogen bonds and occupying the central position in the dodecahedron. He says it is not necessary that the dodecahedra retain the orientations found in the hydrates. They can be arranged in closest packing arrays resulting in a density of 1.00 gm/cm^3. This particular structure corresponds to a breaking of 16.7% of the hydrogen bonds as compared to ice. Danford and Levy[50,58] have found excellent agreement for the radial distribution

computed for a structure similar to Pauling's model when compared with the X-ray data over the whole range of scattering angles. Hasted[59] has pointed out that there are several small peaks in the data obtained by Danford and Levy that can be explained by a structure containing the pentagonal rings present in Pauling's model.

Most of the recent experimental and theoretical work has been concerned with clarification of the problem whether the liquid state of water is to be regarded as a mixture of various structural states existing over distances greater than molecular dimensions, or a continuous distribution of variously fluctuating states of intermolecular bonding. A number of criticisms of the "flickering cluster" theories have been presented in the literature.[42] The assumption of equal spacing for the energy levels of the five species utilized by Nemethy and Scheraga is an over-simplification because the charge-separation effect in the hydrogen bonding may cause the energy levels of the five different molecular species to rise above the energies of levels derived on the assumption of equal spacing and a nonlinear increase in nearest neighbors for each step of bonding may cause unequal contributions to arise in the bonding energy.

Several two-state theories of water structure have been presented.[60-63] Some of these theories picture the liquid as a mixture of two or more polymerically-bonded structures where the degree of polymerization in the

component structures may be large[60] or small.[61] In others, the two forms are regarded as either completely bound or completely unbound.[64] Pople's model explained the maximum density observed at 4°C in terms of some "bending in" of water molecules into the void regions of the ice-like framework of water.[44] His calculation of the radial distribution curve up to 4.5 Å gave results in good agreement with experiment.[49]

The treatment of the liquid as a mixture of tetrahedrally bound molecules in equilibrium with free rotating monomers such as that given by Marchi and Eyring[64] is called the theory of significant structures for liquids. Two approaches are used, the first being a time-averaging of the effective properties of one molecule and the other being a space-averaging of the instantaneous properties exhibited by many molecules over all the space they occupy. Various thermodynamic parameters such as an "effective" characteristic temperature are determined by fitting the averaged partition function to the observed thermodynamic data.

The fact that nonlinear hydrogen bonds which are still significantly bonded can exist is confirmed by the existence of such bonds in compounds such as acetic acid where the intermolecular hydrogen bonds are linear and the intramolecular hydrogen bonds are bent.[91] The existence of bent bonds in known structures casts some doubt as to the accuracy of any

theory which does not allow bent bonds to exist. A continuous distribution of states would seem to be possible in a model allowing for a distribution of hydrogen bond energies and geometries. This continuum model considers the average strength of hydrogen bonds in the liquid to be weaker than in ice as a result of irregular distortion and elongation, both of which increase with temperature.

Falk and Ford[64] present several convincing arguments for a preference of the continuum model over the structered cluster models. They utilize the behaviour of the (O-H) stretching vibration frequencies with changing temperature to determine the strength and extent of hydrogen bonding in the liquid. The frequency of (O-H) stretching vibrations is known to decrease in a regular manner with the strength of hydrogen bonding.[65] Thus, the Raman and infrared spectra of liquid water provide a means of identifying the proper model.

The model presented by Sparnaay[66] is an attempt to rectify the various deficiencies of the above models. His theory is actually a combination of the continuum model of Pople and the cluster model of Nemethy and Scheraga. Sparnaay allows bending of the bonds up to some definite angle, and then defines the bond to be broken if the angle of bending exceeds the maximum allowed angle. This model considers liquid water as having a distorted ice structure in clusters of various sizes.

Deragin and co-workers[67] have reported a number of

anomalous properties of water condensed in quartz capillaries from an incompletely saturated water vapor atmosphere. The properties of this type of water include an equilibrium vapor pressure smaller than that of normal water, $p_a=0.93p_s$, a density of 1.2-1.3 gm/cm^3, a viscosity of about fifteen times that of normal water, and an average coefficient of thermal expansion nearly 1.5 times the normal value. The values of the equilibrium vapor pressure are independent of the radius of the capillaries indicating that the anomalous behaviour is due to a volume phase differing from the normal liquid phase. By subjecting the column of anomalous water to evaporation, its anomalous character is increased, and by heating the water to 400 - 500 °C in a sealed quartz capillary and then recondensing, the anomalous properties are preserved. It has been suggested[93] that this anomalous form of liquid water might always be present at the surface of the liquid phase; however, the fact that one is able to fractionate the anomalous form from the normal form would seem to disprove this postulate. Since the anomalous form is more stable than normal water, one might wonder why all liquid water is not of the anomalous form, unless the quartz capillaries are directly involved as a catalyst in the formation of anomalous water. Any theoretical treatment of the water problem should allow for a unified treatment of the anomalous water structure.

In summary, the most attractive model of liquid water

is one similar to that proposed by Sparnaay in which clusters of various sizes may be present with hydrogen bonding in various states of elongation and distortion allowed to exist. Such a structure could be described as a continuum model, because the definition of exactly what constitutes a "broken" hydrogen bond would determine the size distribution of clusters. This is the type of bonding to be assumed in the clustering of water molecules in the vapor state, the molecules will tend to hydrogen-bond to one another in the tetrahedral coordination as observed in ice, but they are allowed to bend as well as stretch in order to maintain as much spherical symmetry as possible in the clustering process.

II-2. The Structure of Ice. The crystal structure of ice has been examined many times, yet there are still unanswered questions concerning this common solid. Detailed reviews of the structure, electrical properties, X-ray scattering, theoretical structure, and entropy have been presented by Owston,[68] Bjerrum,[69] Lonsdale,[70] and Pauling.[54] Ice has several known crystal structures similar in character to those of silica (SiO_2). The form which is stable between -80 °C and 0 °C is a hexagonal structure which is similar to that observed in tridymite, a form of silica. Normally, when one speaks of ice, the reference is to this hexagonal, tridymite like, ice-I. The crystal structure is a hexagonal lattice as shown in Figure 8, where each oxygen atom is

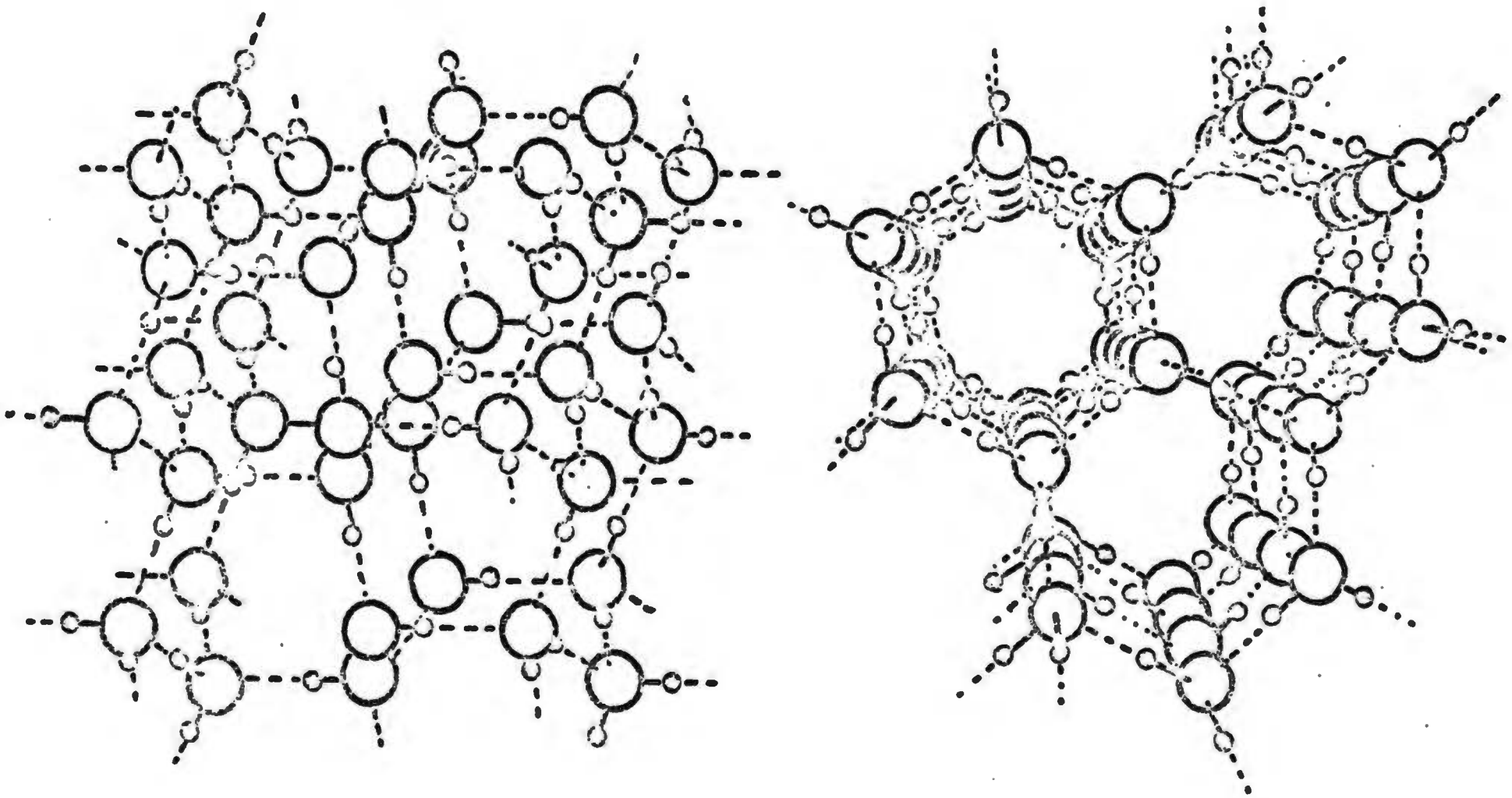

Figure 8. Water Molecules in Ice Crystal are Arrayed in a Hexagonal Pattern, Viewed From the Side (left) and From the Top (right). The Hydrogen Atoms are Oriented at Random, Even at Very Low Temperatures.

surrounded tetrahedrally by four other oxygen atoms. The hydrogen atoms are distributed randomly between the oxygens even at low temperatures. The structure may be pictured as a crinkled layer of hexagonal rings in the (001) planes separated by hydrogen bonds in the direction of the c-axis. Another structure for ice I has been reported with a cubic unit cell. This cubic structure is the same as that of diamond. The proper identification of these two forms of ice are ice Ih and ice Ic for the hexagonal and cubic forms respectively. Bertie and Whalley[71] have investigated the far-infrared spectra in the range 50-360 cm^{-1} of ice Ih and ice Ic made from H_2O and D_2O, and of vitreous ice made from H_2O. There is no detectable difference between the spectra of ice Ih and ice Ic. Giguere and Arraudeau[72] likewise found no difference between the spectra in the range 170-4000 cm^{-1}.

Bertie and Whalley[71] determined that the far-infrared spectrum for these forms of ice can be interpreted as primarily due to translational vibrations which can be represented by replacing the hydrogen bond with a spring with a force constant of $1.74\text{-}1.90 \times 10^4$ dyn cm^{-1}. To obtain the best fit with the observed spectral lines, they introduced a bending force constant to represent the coupling between the librational motion and the vibrations.

The librational contribution is not as well understood. A broad band with a maximum near 840 cm^{-1} has generally been attributed to hindered rotations.[71] Since this band is quite

broad, the resolution is not sufficient to separate the different frequency components. Each molecule is surrounded by four molecules with the dipoles tending to point in nearly the same direction as that of the surrounded molecule (Figure 5). It is shown in Appendix III that the dipole-dipole interaction per pair of adjacent molecules averages to -0.75 kcal/mole so that the total nearest neighbor dipole-dipole interaction energy in ice is -3.00 kcal/mole. This suggests that the predominate librations are probably about the molecular dipole axis. Since no definite value for this librational frequency is available, we choose to approximate the bonding scheme by a two-dimensional model with librations about an axis perpendicular to the plane containing the bonds. If the nearest neighbor molecules are held fixed, the net restoring torque due to a rotation through angle θ is equal in magnitude to $4k_\theta a^2\theta$, where a is the intermolecular separation and k_θ is the torsional force constant. The equation of motion is then

$$I\frac{d^2\theta}{dt^2} = 4\ k_\theta a^2\theta$$

or

$$ma^2\ \frac{d^2\theta}{dt^2} = 4\ k_\theta a^2\theta$$

The solutions to this equation of motion are sinusoidal with angular frequency $\omega = 2(k_\theta/m)^{1/2}$. Since no better value for

the librational frequency is available, the peak value of 840 cm^{-1} is used resulting in the value of 420 cm^{-1} for the bending frequency of a singly bonded molecule. This corresponds to a value of 1.75×10^3 dyn cm^{-1} for k_θ. The proper torsional force constant would be somewhat larger due to the non-planar configuration; however, since no reliable value for the librational frequency is available, the above approximation is used in the present work.

II-3. The Structure of Water Vapor. Water vapor has been considered to be primarily made up of monomers with some association present. It is a mixture of molecular clusters consisting of monomers, dimers, trimers, etc. The nonideal behaviour of the vapor may be accounted for by the change in the total number of particles due to association. One cannot gain information concerning the clusters in the vapor because the cluster concentration is extremely small in the undersaturated vapor. Hall and Dowling[35] have been successful in attributing the observed far-infrared spectrum of water vapor to the pure rotational spectrum of monomers. One cannot expect to gain information about dimers or trimers from the infrared spectrum, because any lines present in the spectrum would be hidden in the noise of the background.

Since water vapor is an associated gas, one might gain information about the clusters if the cluster structure and bond energies were known. Fortunately, the hydrogen bonding scheme of the water molecule provides simplification which is needed to make possible a satisfactory theory for the clustering

process in the vapor.

The equation of state may be developed in terms of the concentration equilibrium constants. This sort of development has been discussed many times; for example, the results reported by Woolley[92] include an expression for the equation of state of the vapor in virial form. In this sort of approach to the problem, the non-ideal behaviour of the water vapor can be accounted for by considering the vapor as an ideal mixture of molecular clusters A_g ($g=1,2,3,\ldots$), subject to a set of reactions[74]

$$A_1 + A_1 \rightleftarrows A_2$$
$$A_2 + A_1 \rightleftarrows A_3$$
$$\ldots\ldots\ldots\ldots$$
$$A_{g-1} + A_1 \rightleftarrows A_g$$

which result in an equilibrium distribution of clusters with the g-cluster equilibrium constant, $K_g = n_g/(n_1)^g$. n_g is the equilibrium concentration for the g-clusters. The total number of molecules of the gas is related to the number of g-clusters, N_g, by

$$N = \sum_g g N_g$$

Since each g-cluster may exist in several different configurations, N_g includes clusters of all configurations containing g molecules.

If we assume that the volume occupied by the clusters is negligible compared to the volume available and each subsystem of g-clusters behaves as an ideal gas, i.e. $p_g = n_g kT$, then

$$p/kT = \sum_g n_g = \sum_g K_g (n_1)^g \quad .$$

Since

$$N/V = n = \sum_g g n_g = \sum_g g K_g (n_1)^g \quad ,$$

dividing p/kT by n, yields

$$p/nkT = [\sum_g K_g (n_1)^g]/[\sum_g g K_g (n_1)^g]$$

or

$$p/nkT = 1 - K_2 n_1 + (2K_2^2 - 2K_3) n_1^2 + (-4K_2^3 + 7K_2K_3 - 3K_4) n_1^3 + \ldots \quad .$$

By inversion of the series $n = \sum_g g K_g (n_1)^g$, a series for n_1 is obtained

$$n_1 = n - 2K_2 n^2 + (8K_2^2 - 3K_3) n^3 + \ldots \quad .$$

Substitution of this series for n_1 in the expression for p/nkT yields an equation for p/kT in a power series of n,

$$p/kT = n - K_2 n^2 + (4K_2^2 - 2K_3) n^3 + (-20K_2^3 + 18K_2K_3 - 3K_4) n^4 + \ldots \quad .$$

Inversion of this series gives

$$n = p/kT + K_2 (p/kT)^2 + (-2K_2^2 + 2K_3)(p/kT)^3 + \ldots \quad ,$$

which may be used to obtain an expression for pV/NkT:[74]

$$pV/NkT = 1 - K_2(p/kT) + (3K_2^2 - 2K_3)(p/kT)^2 + (-10K_2^3 + 12K_2K_3 - 3K_4)(p/kT)^3 + \ldots$$

This equation provides a means of estimating the concentration equilibrium constants for an associated vapor.

Keyes[73] has determined the coefficients up to the third order in p/kT by terminating the series at $(p/kT)^3$ and obtaining the best fit with the observed p-V-T characteristics of undersaturated water vapor in the temperature range 0°C - 150°C. The values determined by Keyes should give good values for the second equilibrium constant and fair results for the third equilibrium constant, because errors in the K_2 coefficient will contribute to errors in the calculation of the third equilibrium constant since K_2 is squared in the third coefficient. If the fourth equilibrium were determined from Keyes' equation of state, it would not be very accurate at all. Not only does K_2^3 and K_2K_3 occur, but the termination of the series contributes to errors in the value obtained for K_4. The results of Keyes' work are indicated in Table II. The values of the second, third, and fourth equilibrium constants as calculated from Keyes' equation of state for water vapor are given in Table III. The vapor cluster model developed in this study must be capable of predicting these equilibrium constants which have been obtained from experimental observation. In other words, this data

TABLE II

The Coefficients of the Pressure Series for the Equation of State of Water Vapor as Reported by Keyes.[73]

$$pv/RT = 1 + B_1(p/RT) + B_2(p/RT)^2 + B_3(p/RT)^3$$

T (°C)	$-B_1$ ($cm^3 gm^{-1}$)	$-B_2$ ($cm^3 gm^{-1}$)^2	$-B_3$ ($cm^3 gm^{-1}$)^3
0	102.93	2.89×10^5	2.83×10^7
10	84.34	1.52×10^5	1.20×10^7
20	70.27	0.85×10^5	0.55×10^7
30	59.42	4.98×10^4	0.27×10^7
40	50.89	3.04×10^4	0.14×10^7
50	44.08	1.93×10^4	7.28×10^5
60	38.57	1.25×10^4	4.06×10^5
70	34.04	0.85×10^4	2.37×10^5
80	30.29	5.92×10^3	1.42×10^5
90	27.14	4.21×10^3	0.88×10^5
100	24.48	3.06×10^3	5.53×10^4
110	22.20	2.27×10^3	3.57×10^4
120	20.24	1.71×10^3	2.36×10^4
130	18.54	1.31×10^3	1.69×10^4
140	17.06	1.02×10^3	1.08×10^4
150	15.75	0.81×10^3	0.75×10^4

The units of volume are expressed in cubic centimeters per gram and the units of the gas constant, R, are in ergs per gram per degree Kelvin in Keyes' work.

TABLE III

The Values of the Second, Third, and Fourth Equilibrium Constants as Determined from the Equation of State of Keyes.*

T (°C)	K_2 (cm^{-3})	K_3 (cm^{-6})	K_4 (cm^{-9})
0	3.079×10^{-21}	1.44×10^{-40}	1.93×10^{-60}
10	2.523×10^{-21}	7.76×10^{-41}	8.38×10^{-61}
20	2.102×10^{-21}	4.47×10^{-41}	3.94×10^{-61}
30	1.777×10^{-21}	2.49×10^{-41}	1.83×10^{-61}
40	1.522×10^{-21}	1.71×10^{-41}	1.05×10^{-61}
50	1.319×10^{-21}	1.12×10^{-41}	5.80×10^{-62}
60	1.154×10^{-21}	7.59×10^{-42}	3.36×10^{-62}
70	1.018×10^{-21}	5.36×10^{-42}	2.04×10^{-62}
80	0.906×10^{-21}	3.88×10^{-42}	1.29×10^{-62}
90	0.812×10^{-21}	2.87×10^{-42}	8.33×10^{-63}
100	0.732×10^{-21}	2.17×10^{-42}	5.54×10^{-63}
110	0.664×10^{-21}	1.68×10^{-42}	3.81×10^{-63}
120	0.605×10^{-21}	1.31×10^{-42}	2.64×10^{-63}
130	0.555×10^{-21}	1.05×10^{-42}	1.91×10^{-63}
140	0.510×10^{-21}	8.46×10^{-43}	1.38×10^{-63}
150	0.471×10^{-21}	6.59×10^{-43}	9.61×10^{-64}

* The values of the concentration equilibrium constants at the various temperatures are calculated using the equation of state developed on Page 37 in conjuction with the equation of state given in Table II.

should provide a test of the theory for the first few clusters.

II-4. Summary of Concepts to be Utilized in This Study. The basic concept to be utilized in this work is the strong tendency of water molecules to form hydrogen bonded clusters as evidenced in the various physical properties of liquid water. The vibrational frequencies for stretching and bending of the hydrogen bonds are determined by using the force constants which are supported by the infrared and Raman spectra of ice I and liquid water. The presence of actual physical clusters in the vapor enables one to develop an expression for the vapor partition function.

The empirical equation of state developed by Keyes[73] in conjunction with the above information provides the necessary information to estimate the temperature dependence of the dimer and trimer binding energies. These binding energies have contributions due to nearest and second nearest neighbor interactions enabling one to estimate the binding energies for larger clusters.

CHAPTER III

DEVELOPMENT OF STATISTICAL METHOD AND DETERMINATION OF HYDROGEN BOND ENERGIES

The partition function for a system of molecules involved in chemical association or physical clustering in the vapor phase can be evaluated if the cluster binding energies and internal vibrational modes are known. In this chapter, the expression for the partition function is developed and the concentration equilibrium constants are found in terms of the partition function. It is shown that the partition function is strongly dependent on the cluster structure and energy. In order to develop a clustering model and to determine the cluster binding energies, the properties of water reviewed in Chapter II are utilized. A general expression for the cluster interaction energy is developed and the vapor phase clustering model is presented in Chapter IV.

Several approximations must be made in the development, but the resulting values found for the dimer binding energy provide excellent agreement with values calculated by various workers[79-81] using several different quantum mechanical techniques. This agreement provides the necessary support for the assumptions made in this calculation. There are no known accurate calculations for the trimer interaction energy, so no comparison with quantum mechanical theory is available. It is hoped that such calculations will be

available for comparison in the near future. Otherwise, one must proceed assuming the trimer energy is correct.

III-1. Statistical Thermodynamic Considerations. The equilibrium constants, K_g, can be related to the cluster partition function which, in turn, requires a detailed knowledge of the cluster structure and intermolecular forces. This information may be determined for small clusters using the equation of state for water vapor. In the undersaturated vapor the extent of molecular association is relatively small and contributions to the equation of state is due mostly to small clusters.

The general expression for the partition function of a system consisting of N particles is[74]

$$\frac{1}{N!\ h^{3N}} \int_{-\infty}^{\infty} \cdots \int_{V} \exp[-E(\vec{r}_1 \cdots \vec{r}_N, \vec{p}_1 \cdots \vec{p}_N)/kT] d\vec{r}_1 \cdots d\vec{r}_N d\vec{p}_1 \cdots d\vec{p}_N$$

where h is Planck's constant, E is the total energy of the system, $\vec{r}_i$ are the position coordinates of the molecules, and $\vec{p}_i$ are the momenta. The integrations over the momenta are from $-\infty$ to $+\infty$ while the coordinates of position span the volume V of the system. The energy, E, is separable in terms of the momenta, but not in terms of the position coordinates,[74]

$$E = \sum_i p_i^2/2m + U(\vec{r}_i \cdots \vec{r}_N) \quad .$$

In the physical cluster model, the interactions between

two molecules not in the same cluster are neglected, so that the potential energy, U, may be separated into independent terms, one for each cluster. The position coordinates in a given term are those belonging to the molecules in the cluster to which the term corresponds. The energy may then be written as a sum over the N_g clusters.[74]

$$E = \sum_g \{N_g[\sum_{i=1}^{g} p_{ig}^2/2m + U_g(\vec{r}_{1g}\ldots\vec{r}_{gg})]\}$$

or

$$E = \sum_g N_g E_g \quad .$$

The N! in the denominator of the expression for the partition function on page 42 is due to the fact that the water molecules are not distinguishable, and the integration is performed as if the molecules were distinguishable. The number of ways N indistinguishable molecules may be partitioned among a particular distribution of clusters (N_g of size g) is[74]

$$\frac{N!}{\prod_g (g!)^{N_g} N_g!}$$

where g! counts permutations within a g-cluster and N_g! counts permutations of identical clusters. Since the integrations in the partition function are performed over all of these indistinguishable configurations, the proper value is obtained by performing the integration once for the distribution and then multiplying by the above factor,

and summing over all possible distributions. The partition function may then be expressed as[74]

$$Q = \sum_{N_g} \prod_{g} \left\{ \frac{1}{N_g!} \left[\frac{1}{g!\, h^{3g}} \int_{-\infty}^{\infty} \cdots \int_{V} \exp(-E_g/kT)\, dr_{1g} \cdots dp_{gg} \right]^{N_g} \right\}$$

or

$$Q = \sum_{N_g} \prod_{g} \frac{1}{N_g!} \left(\frac{Q_g}{g!} \right)^{N_g} = \sum_{N_g} \Xi_{Ng}$$

where Q_g is the single g-cluster partition function.

The individual cluster partition function contains contributions due to bulk cluster translation, Q_{gt}; bulk rotation, Q_{gr}; internal vibrations and rotations, Q_{gi}; electronic energy levels, Q_{ge}; and nuclear energy levels, Q_{gn}; that is[74]

$$Q_g = Q_{gt} Q_{gr} Q_{gi} Q_{ge} Q_{gn} \exp(-E_g^o/kT) \quad .$$

Here, E_g^o is the cluster binding energy measured with respect to the energy when all molecules are completely separated.

The cluster translational contribution is given by [74]

$$Q_{gt} = V' (2\pi gmkT)^{3/2} h^{-3} \quad ,$$

where V' is the total volume available to the vapor. For the present study, the volume occupied by the clusters is considered negligible compared to the volume of the system; hence, V' ≈ V. The cluster rotational contribution to the partition function is given by [74]

$$Q_{gr} = 8\pi^2(2\pi kT)^{3/2} (A_g B_g C_g)^{1/2} / \sigma_g h^3 ,$$

where A_g, B_g, and C_g are the principal moments of inertia and σ_g is the rotational symmetry number of the g-cluster. This expression is valid for the temperature range of interest in this study. The internal vibrational and rotational contribution is expressed as

$$Q_{gi} = (g!/ \prod_s X_s!)\, r_g \prod_m f_{gm} ,$$

where r_g represents the number of different orientations possible for the molecules in the g-cluster. This factor is necessary because the hydrogen atoms have four sites available and one would expect a random distribution for these positions subject to the particular structure considered. The factor $(g!/ \prod_s X_s!)$ is the number of permutations of the g molecules distributed among indistinguishable positions in the cluster, where $g = \sum_s X_s$, and X_s is the number of molecules in the equivalent positions s (see Figure 10). The terms f_{gm} are the internal vibrational and rotational contributions to the cluster partition function, given by[74]

$$f_{gm} = \begin{cases} (8\pi^3 I_{gm} kT)^{\frac{1}{2}}/\sigma_{gm} h^2, & \text{(free rotation about a single hydrogen bond)} \\ \sum_n^{N_m} \exp(-E^n_{gm}/kT), & \text{(vibrations and/or librations)} \end{cases}$$

where n is the quantum number identifying the energy levels

allowed in the vibrational and librational states, I_{gm} is the moment of inertia of a molecular group about a single hydrogen bond. The nuclei are assumed to be in the same ground states as the separate molecules and the shift in electronic ground states is accounted for in the interaction potential energy such that $Q_{gn} = (Q_{1n})^g$ and $Q_{ge} = (Q_{1e})^g$. Earlier statistical calculations have neglected the electronic shift completely,[22] this work considers the influence of bond strength on the (O-H) vibrational levels accounting for part of this shift.

Letting

$$q_g = (Q_{gt}Q_{gr}Q_{gi}/Vg!)\exp(-E_g^o/kT)$$

and using the expressions for Q and Q_g above, the partition function for the system can be written

$$Q = \sum_{N_g} (Q_{1e}Q_{1n})^N \prod_g (Vq_g)^{N_g}/N_g! = \sum_{N_g} \Xi_{N_g}$$

The equilibrium distribution among the clusters is determined by finding the maximum term in the above series subject to the condition that the total number of molecules, N, be conserved.[74] This may be accomplished by maximizing $\ln \Xi_{N_g}$,

$$\Delta \ln \Xi = \sum_g \frac{\partial \ln \Xi}{\partial N_g} \Delta N_g = \sum_g [\ln(Vq_g) - \frac{\partial \ln(N_g!)}{\partial N_g}]\Delta N_g = 0$$

or, applying Stirling's approximation, $\ln(X!) = X \ln X - X$,

$$\sum_g [\ln(Vq_g) - \ln N_g] \Delta N_g = \sum_g \ln(Vq_g/N_g) \Delta N_g = 0 .$$

To determine the equilibrium concentration of the g-clusters as a function of the number of monomers, one inserts $\Delta N_1 = -g$ and $\Delta N_g = +1$ into the above expression with all other $\Delta N_g = 0$, and obtain

$$-g \ln(q_1 V/N_1) + \ln(q_g V/N_g) = 0$$

or, since $n_g = N_g/V$ and $K_g = n_g/n_1^g$,

$$K_g = q_g/(q_1)^g \quad .$$

This expression is valid if one may represent the vapor as a system of physical clusters and the total volume occupied by the clusters is negligible when compared to the volume of the system under consideration. For cloud chamber experiments this should be a fair approximation until catastrophic condensation is initiated. The errors introduced by these approximations are certainly smaller than those introduced by assuming bulk liquid properties for small clusters. The statistical mechanics of the molecular clustering process should be able to overcome the difficulties of the current nucleation theories in spite of these small errors.

Thus, one has an expression for the concentration equilibrium constant which requires the detailed knowledge of the structure, binding energy, and excitation energy levels of the various g-clusters.

III-2. Assignment of Internal Energy Levels. The empirical data needed to calculate the equilibrium constants, K_g, includes the cluster binding energy, E_g^o; the vibrational energy levels, E_{gm}^n, B_o^1, E_o^g; the cluster moments of inertia, A_g, B_g, C_g; and the moments of inertia for internal rotations, I_{gm}. These quantities are strongly dependent on the configuration characteristics of each type of cluster.

The cluster binding energy provides the initial difficulty, because there has been some disagreement among the various published calculations of the dimer bond energy. The larger clusters will include energy terms due to the coupling through multiply bonded molecules, and the second nearest neighbor interaction energy in directions away from the direction of the hydrogen bond is not available. The procedure in this work is to determine the dimer and trimer binding energies through the use of the empirical concentration equilibrium constants of Table III, page 39. In order to accomplish this, one solves for E_g^o in the expression defining q_g on page 47 and utilizes the fact that $K_g = q_g/(q_1)^g$ to obtain

$$E_g^o = kT \ln[Q_{gt}Q_{gr}Q_{gi}/VK_g(q_1)^g g!] \quad .$$

The cluster librational and vibrational energy levels, E^{o}_{gm}, can be estimated from the observed frequencies in the infrared and Raman spectrum of ice I. The stretching force constant reported by Bertie and Whalley[71] is 1.74-1.90x10^{4} dyn cm^{-1}. Calculations based on both 1.74x10^{4} dyn cm^{-1} and 1.90x10^{4} dyn cm^{-1} are made and the deviation between the results is smaller than the experimental error in the empirically determined equilibrium constants. As indicated in section II-2, the librational frequencies have not been resolved well enough to assign an accurate value to the bending force constant. The approximate value of 1.75x10^{3} dyn cm^{-1} is used in the calculations, and this is certainly the most questionable quantity used in this work. Even the neglect of coupling between stretching and bending vibrations probably introduces a smaller error. The cluster bending and stretching potential energy is written[71]

$$V = (1/2)k_r \sum_{ij} r_{ij}^2 + (1/2)k_\theta a^2 \sum_{ij} \theta_{ij}^2$$

where r_{ij} is the change in the distance between nearest neighbors i and j, a is the equilibrium nearest neighbor distance, and θ_{ij} is the net bending angle for the hydrogen bond. The amplitude of vibration is assumed sufficiently small so that the coupling between the translational vibrations and librations can be neglected. Free rotation is allowed about a single hydrogen bond.

The coordinates necessary for the dimer are indicated

in Figure 9a. Using the approximate general expression for the stretching and bending potential energy, the Lagrangian for the dimer is written

$$L = \tfrac{1}{2}m(\dot{x}^2 + \dot{y}^2) + \tfrac{1}{2}ma^2(\dot{\theta}^2 + \dot{\phi}^2) - \tfrac{1}{2}k_r(x + y)^2 - \tfrac{1}{2}k_\theta a^2(\theta + \phi)^2,$$

with the resulting equations of motion

$$\begin{aligned} m\ddot{x} + k_r(x + y) &= 0 \\ m\ddot{y} + k_r(x + y) &= 0 \\ m\ddot{\theta} + k_\theta(\theta + \phi) &= 0 \\ m\ddot{\phi} + k_\theta(\theta + \phi) &= 0 \end{aligned} \quad .$$

The solutions to this set of equations are $\omega_r = (2k_r/m)^{\frac{1}{2}}$ and $\omega_\theta = (2k_\theta/m)^{\frac{1}{2}}$ for the stretching and bending modes respectively. The energy levels are approximated by the simple harmonic energy levels, giving

$$E^n_{gm} = \hbar\omega_m\,(\tfrac{1}{2} + n) \;;\quad n = 0,1,2,\ldots \quad .$$

The trimer energy levels may be estimated by the same technique. The necessary coordinates are indicated in Figure 9b. The approximate trimer stretching and bending potential energy is

$$V = \tfrac{1}{2}k_r(x_1 + x_2\cos\tfrac{1}{2}\alpha + y_2\cos\tfrac{1}{2}\alpha)^2 + \tfrac{1}{2}k_r(-x_2\sin\tfrac{1}{2}\alpha + y_2\sin\tfrac{1}{2}\alpha + x_3)^2 + \tfrac{1}{2}k_\theta a^2(\theta_1 - \theta_{21})^2 + \tfrac{1}{2}k_\theta a^2(\theta_{22} - \theta_3)^2 \,,$$

where $\alpha = \alpha_o + \theta_{22} - \theta_{21}$ and α_o is the equilibrium angle between hydrogen bond directions, 109.5°.

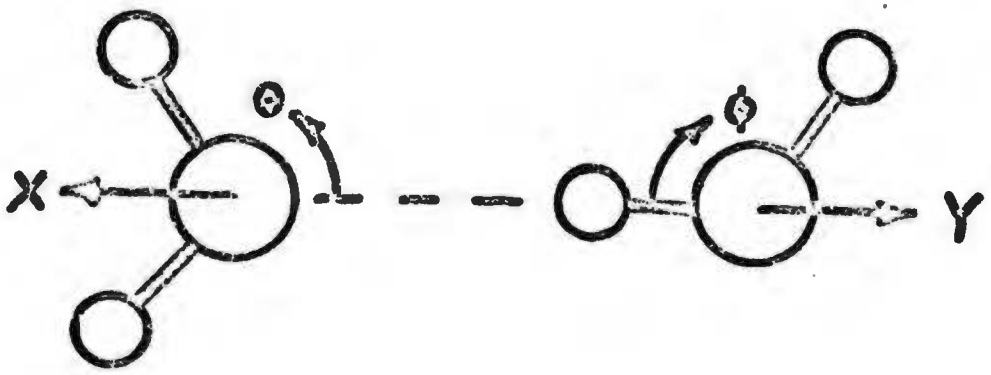

a. Internal Coordinates of the Water Dimer.

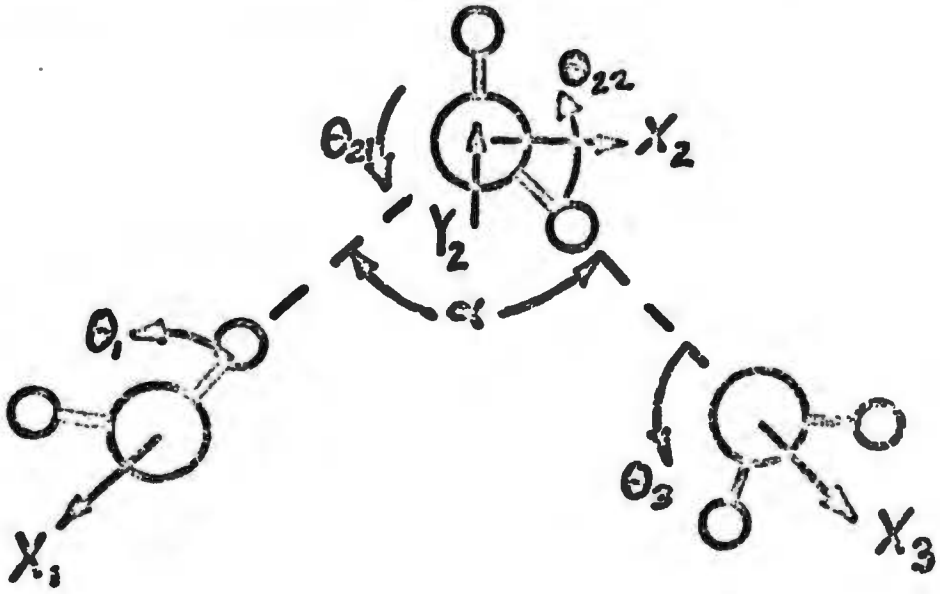

b. Internal Coordinates of the Water Trimer.

Figure 9. The Internal Coordinates of the Water Trimer and Dimer.

The Lagrangian is then

$$L = \tfrac{1}{2}m(\dot{x}_1^2 + \dot{x}_2^2 + \dot{y}_2^2 + \dot{x}_3^2) + \tfrac{1}{2}ma^2(\dot{\theta}_1^2 + \dot{\theta}_{21}^2 + \dot{\theta}_{22}^2 + \dot{\theta}_3^2) +$$
$$- \tfrac{1}{2}k_r(x_1 + x_2\cos\tfrac{1}{2}\alpha + y_2\cos\tfrac{1}{2}\alpha)^2 - \tfrac{1}{2}k_r(-x_2\sin\tfrac{1}{2}\alpha + y_2\sin\tfrac{1}{2}\alpha +$$
$$+ x_3)^2 - \tfrac{1}{2}k\,a^2(\theta_1 - \theta_{21})^2 - \tfrac{1}{2}k\,a^2(\theta_{22} - \theta_3)^2$$

resulting in the equations of motion (neglecting the coupling terms; i.e., θ_{22}, $\theta_{21} \ll \alpha_o$ and x_1, x_2, y_2, $x_3 \ll a$),

$$m\ddot{x}_1 + k_r(x_1 + x_2\cos\tfrac{1}{2}\alpha_o + y_2\cos\tfrac{1}{2}\alpha_o) = 0$$
$$m\ddot{x}_2 + k_r(x_1\cos\tfrac{1}{2}\alpha_o + x_2 - x_3\sin\tfrac{1}{2}\alpha_o) = 0$$
$$m\ddot{y}_2 + k_r[x_1\cos\tfrac{1}{2}\alpha_o + x_2(\cos^2\tfrac{1}{2}\alpha_o - \sin^2\tfrac{1}{2}\alpha_o) + y_2 + x_3\sin\tfrac{1}{2}\alpha_o) = 0$$
$$m\ddot{x}_3 + k_r(-x_2\sin\tfrac{1}{2}\alpha_o + y_2\sin\tfrac{1}{2}\alpha_o + x_3) = 0$$
$$m\ddot{\varepsilon}_1 + k_\theta(\theta_1 - \theta_{21}) = 0$$
$$m\ddot{\theta}_{21} - k_\theta(\theta_1 - \theta_{21}) = 0$$
$$m\ddot{\theta}_{22} + k_\theta(\theta_{22} - \theta_3) = 0$$
$$m\ddot{\theta}_3 - k_\theta(\theta_{22} - \theta_3) = 0 \quad .$$

In Appendix I, the above set of equations is solved with the result that the solutions for the vibration frequencies yield $(k_r/m)^{\frac{1}{2}}$ for the four translational vibration frequencies and $(2k_\theta/m)^{\frac{1}{2}}$ for the four librational frequencies.

The ground state vibrational levels, E_o^l and E_o^g, include the contributions due to the internal vibrations of the water molecules. The frequencies of these vibrations are dependent on the strength of the hydrogen bonds in which each molecule participates. Consequently, the two stretching modes, ν_1

and ν_3, have been observed to shift downward and the bending mode, ν_2, upward, with respect to monomeric molecules in the vapor state. The values of the frequencies of a monomer are, respectively, $\nu_1 = 3652\ cm^{-1}$, $\nu_2 = 1592\ cm^{-1}$, and $\nu_3 = 3756\ cm^{-1}$ while the corresponding values in ice I are $\nu_1 = 3210\ cm^{-1}$, $\nu_2 = 1640\ cm^{-1}$, and $\nu_3 = 3302\ cm^{-1}$. Furthermore, hydrogen bond lengths ranging from 2.49 Å to 3.36 Å have been reported in various compounds and experimental evidence implies that a hydrogen bond length determined in one phase cannot, in general be assumed to apply in other phases. Consequently, since the internal vibration frequencies depend directly on the bond strength which, in turn, is a function of the bond length, and due to the lack of experimental data of the actual bond length for the water dimer and trimer in the vapor phase, calculations for the dimer are made for several values of the intermolecular separation. The dependence of the intramolecular vibrational frequencies on the bond distance can further be demonstrated by examining the variation of the (O-H) stretching frequency with known hydrogen bond lengths, R(O-H...O), in various hydroxides, as given in Table IV. For ice I, the frequencies of $3210\ cm^{-1}$ and $3302\ cm^{-1}$ at bond length, 2.76 Å, fit well in the general trend indicated by the table. Using the average value of $3256\ cm^{-1}$ for ice I and the other data of Table IV, the following empirical relationship for the shift in the (O-H) stretching frequency is obtained by

means of a graphical fit,

$$\Delta\nu_s = -(1.46 \times 10^9)\, R^{-14.8}\ cm^{-1} \quad .$$

Various values of $\Delta\nu_s$, calculated from this equation are also listed in Table IV. In the clusters, the stretching frequencies of the molecules bonded through an electron pair are assumed to be 3704 cm^{-1}, while those of a molecule bonded through a proton are assumed to be $(3704 + \Delta\nu_s)$ cm^{-1}.

The cluster moments of inertia, A_g, B_g, and C_g also depend upon the length of the hydrogen bond, according to the following relations which are developed in Appendix II,

$$A_2 = B_2 = 5.97 \times 10^{-39}\, R^2 \quad (g\ cm^2)$$
$$C_2 = 3.41 \times 10^{-40} \quad (g\ cm^2),$$

where A_2 and B_2 are the moments of inertia about axes perpendicular to the hydrogen bond axis and C_2 is that about the bond axis. The internal moments of inertia about the bond axis are 1.44×10^{-40} g cm^2 and 1.97×10^{-40} g cm^2. In the trimer, the factor $(A_3B_3C_3)^{\frac{1}{2}}$ is equal to $8.10 \times R^3 \times 10^{-59}$ while there are internal rotations present also.

There is only one way the molecules can be oriented in the dimer so that $r_2 = 1$. In the trimer, there are three possible orientations allowed as indicated in Figure 9 resulting in $r_3 = 3$.

III-3. Calculation of Dimer and Trimer Bond Energies. The dimer and trimer potential energies are calculated using the parameters in Table V. The dimer hydrogen

TABLE IV

Variation of the (O-H) Stretching Frequencies with the Hydrogen Bond Length in Various Hydroxides as Reported by Glemser and Hartert[75] and as Calculated by the Empirical Equation, $\nu = 3704 - (1.46 \times 10^9) R^{-14.8}$ (cm^{-1}).

Compound	ν (O-H), cm^{-1} Observed[75]	ν (O-H), cm^{-1} Calculated	R(O-H...O), Å
α-FeOOH	3049	3022	2.68
γ-FeOOH	3125	3102	2.70
Ice I	3256	3269	2.76
γ-$Al(OH)_3$	3312	3313	2.78
Nd-$(OH)_3$	3473	3494	2.90
La-$(OH)_3$	3473	3494	2.90
Y-$(OH)_3$	3473	3494	2.90

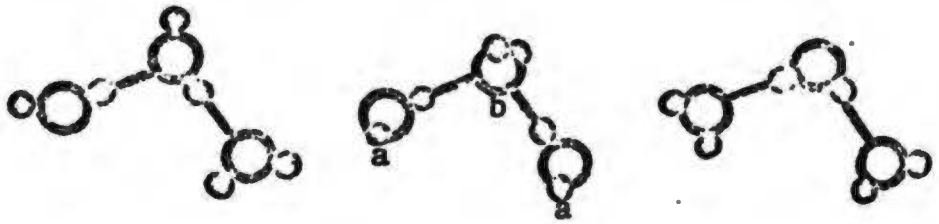

$X_a = 2$

$X_b = 1$

Figure 10. The Three Possible Orientations for the Water Molecules in the Trimer.

TABLE V

Parameters used in the Calculation of the Dimer and Trimer Potential Energies.

$\Gamma_2 = 1$	$\Gamma_3 = 3$
$\sigma_2 = 4$	$\sigma_3 = 2$
$I_{21} = 1.44 \times 10^{-40}$	$I_{31}, I_{32} = 1.50 \times 10^{-40}$
$I_{22} = 1.97 \times 10^{-40}$	$I_{33}, I_{34} = 1.53 \times 10^{-38}$
$\omega_{2m} = 2\,\ell\,(2k_r/m)^{1/2}$	$\omega_{3m} = 4\,\ell\,(k_r/m)^{1/2}$
$2\,\ell\,(2k_\theta/m)^{1/2}$	$4\,\ell\,(2k_\theta/m)^{1/2}$

bond energy is computed for various values of intermolecular separation, R(O-H...O), and at temperatures ranging from 0°C to 150°C. The results are listed in Table VI for R = 2.80 Å, 2.85 Å, and 2.90 Å. It is well known that the hydrogen bond length of a dimer in the vapor phase is greater than that in a condensed phase, such as in crystals. For example, the hydrogen bond length for a vapor dimer of formic acid and acetic acid is 2.73 Å and 2.76 Å, respectively, while in the crystals, these distances are 2.58 Å and 2.61 Å,[76-78] both demonstrating a ratio of 1.06. There is, however, no experimental data for the cluster bond lengths for water in the vapor phase, but one would expect a similar behavior for water vapor and ice. If use is made of the ratio 1.06, the hydrogen bond length for the water dimer in the vapor phase at 0 °C would be 2.92 Å which is very nearly the nearest neighbor distance observed in liquid water on the basis of X-ray diffraction data.[49,50] The distance between nearest neighbors increases from 2.90 Å at 1.5 °C to 3.05 Å at 83 °C. The calculations of cluster potential energy at 2.90 Å should be quite close to the correct values for water vapor.

For purposes of comparison, the hydrogen bond energies calculated by various workers have been listed in Table VII. The calculations by Coulson and Danielsson,[79] McKinney and Barrow,[80] and Grahn[81] are made without the (O-H) ground state vibrations present in the dimer so that their values should compare favorably with the present work if the

TABLE VI

Cluster Binding Energies for the Water Dimer in the Vapor Phase, F_2^o, (kcal/mole).

T (°C)	R = 2.80 Å	R = 2.85 Å	R = 2.90 Å
0	-5.12	-5.22	-5.29
10	-5.12	-5.21	-5.28
20	-5.11	-5.20	-5.28
30	-5.11	-5.20	-5.27
40	-5.10	-5.20	-5.26
50	-5.10	-5.19	-5.26
60	-5.09	-5.19	-5.25
70	-5.09	-5.18	-5.24
80	-5.08	-5.17	-5.24
90	-5.08	-5.17	-5.23
100	-5.07	-5.16	-5.22
110	-5.06	-5.15	-5.21
120	-5.05	-5.14	-5.20
130	-5.04	-5.13	-5.19
140	-5.03	-5.12	-5.18
150	-5.02	-5.10	-5.16

TABLE VII

Dimer Binding Energy as Calculated by Various Authors.

Author(s)	R(O-H...O) (Å)	Bond Energy (kcal/mole)	Remarks
Coulson & Danielsson[79]	2.80	4.4	Pure p-orbitals
	2.90	3.5	
	2.80	6.8	sp^3 hybridization
	2.90	5.3	
McKinney & Barrow[80]	2.80	6.7	Valence-Bond Method
Grahn[81]	2.76	6.5	Electrostatic & Polarization Energies
Rowlinson[82]	2.68	4.4	Stockmayer Method
Coulson[83]	2.80	4.6-12.6	Electrostatic Model
Morokuma & Pedersen[84]	2.68	12.6	SCF-MO-LCAO Method, using Gaussian Orb.
This work	2.90	5.2-5.3	

technique is to prove useful in determining the cluster interaction potential energies. When their results are extrapolated to 2.90 Å, excellent agreement is obtained, with the exception of the results of Morokuma and Pedersen.[84] It should be noted that Rowlinson's results[82] are obtained by assuming the Stockmayer potential and solving for the necessary parameters to yield the observed virial coefficients. Since a form for the potential is assumed, the bond strength and the position of the potential minimum is not necessarily that of the actual potential.

The calculations for the trimer are made only at the hydrogen bond length of 2.90 Å because of the excellent agreement for the dimer calculation. These results are indicated in Table VIII.

III-4. Determination of Dependence of the Binding Energy on the Number of Nearest and Second Nearest Neighbors. The cluster Binding energies indicated in Tables VI and VIII include the dipole-dipole interactions of the nearest neighbors. Since the orientations of nearest neighbors will vary from position to position, the dipole-dipole interactions will have to be removed from the trimer and dimer energies in order to obtain the dependence of the energy on coupling through multiply bonded molecules and the second neighbor interactions. The average dipole-dipole interactions for the dimer are calculated in Appendix III with the results that the dimer dipole-dipole contribution to the energy is

TABLE VIII

Trimer Binding Energies, E_3^o, Caculated Using the Parameters Listed in Table V. The Hydrogen Bond Length, R(O-H...O), is Assumed to be 2.90 Å.

T (°C)	$-E_3^o$ (kcal/mole)
0	8.58
10	8.37
20	8.17
30	7.93
40	7.79
50	7.60
60	7.42
70	7.24
80	7.07
90	6.90
100	6.73
110	6.56
120	6.39
130	6.23
140	6.06
150	5.86

determined to be - 0.748 kcal/mole and the average trimer dipole-dipole contribution is - 2.24 kcal/mole. TABLE IX lists the dimer and trimer binding energies exclusive of dipole-dipole contributions, E_h and $2E_h + E'$. The energy E' includes all contributions due to coupling through the molecule participating in two hydrogen bonds in the trimer and the second neighbor interactions. The values of E_h and E' may be represented quite well by linear functions of temperature as indicated in Figure 11. The temperature dependence thus determined is expressed as

$$E_h = -4.788 + (8.667 \times 10^{-4})\, T(^{\circ}K) \quad \text{(kcal/mole)}$$

and

$$E' = -1.680 + (1.640 \times 10^{-2})\, T(^{\circ}K) \quad \text{(kcal/mole)}.$$

In order to obtain a workable expression for the cluster binding energy, a linear dependence on the number of hydrogen bonds, α, and second nearest neighbor pairs, β, is assumed, resulting in

$$E_g^o = \alpha\, E_h + \beta\, E' + E_g^{d\text{-}d}$$

where $E_g^{d\text{-}d}$ represents the net dipole-dipole contribution to the cluster binding energy in the g-cluster. For the dimer and the trimer, the temperature dependence of the binding energy is then

$$E_2^o = E_h + 0.748 \text{(kcal/mole)}$$

or

TABLE IX

Dimer and Trimer Binding Energies Exclusive of the Dipole-Dipole contributions.

T (°C)	Dimer $-E_h = -E_2^o - 0.75$ (kcal/mole)	Trimer $-2E_h - E' = -E_3^o - 2.24$ (kcal/mole)
0	4.54	6.34
10	4.53	6.13
20	4.53	5.93
30	4.52	5.69
40	4.51	5.55
50	4.51	5.36
60	4.50	5.18
70	4.49	5.00
80	4.49	4.83
90	4.48	4.66
100	4.47	4.49
110	4.46	4.32
120	4.45	4.15
130	4.44	4.00
140	4.43	3.82
150	4.41	3.62

E_h is the single hydrogen bond binding energy exclusive of the dipole-dipole energy.

E' is the second nearest neighbor binding energy exclusive of the dipole-dipole energy.

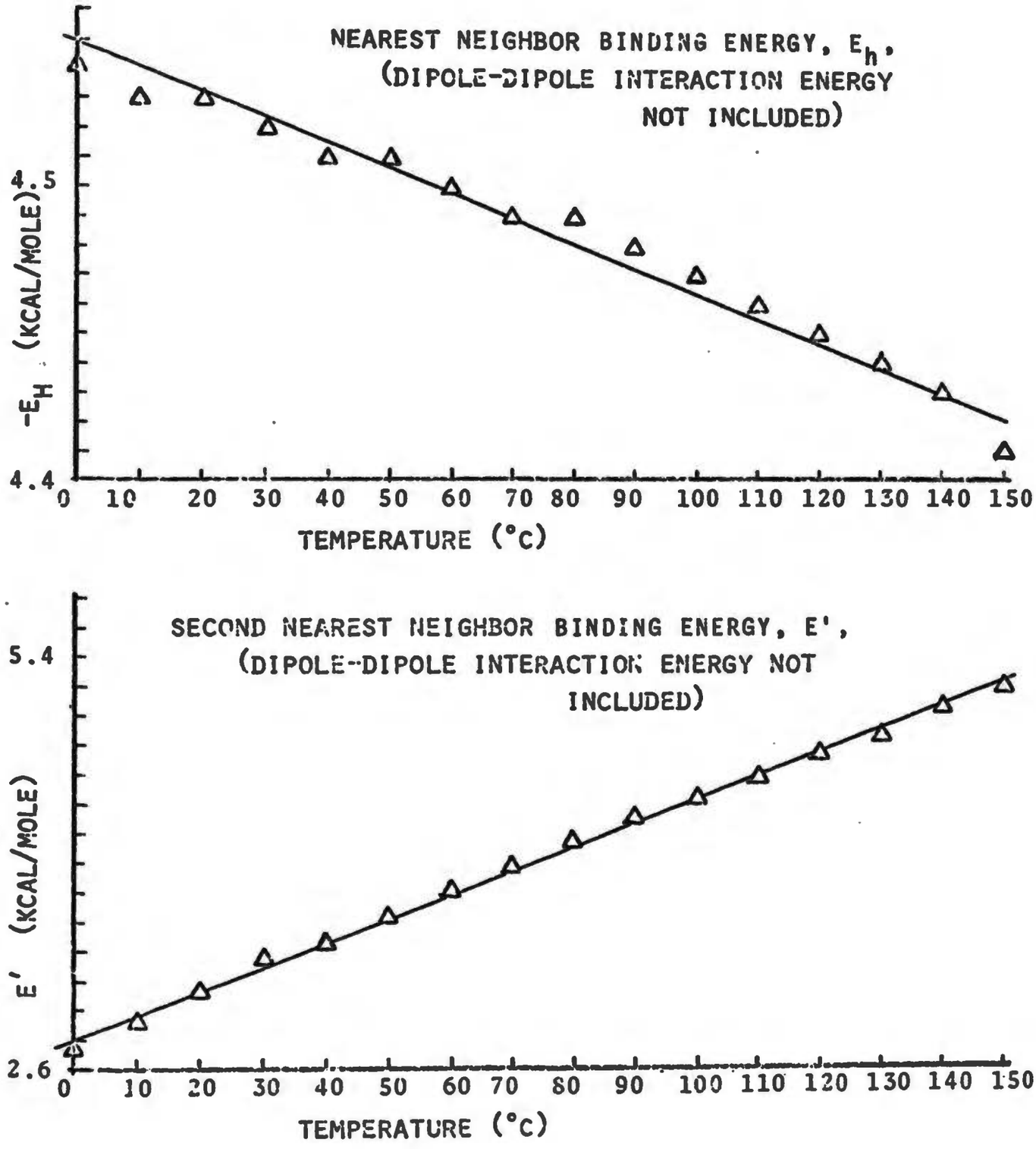

Figure 11. Nearest Neighbor Binding Energy, E_h, and the Second Nearest Neighbor Binding Energy, E'. The Δ points represent values calculated from Table VIII and the solid lines are the plots of E_h and E' as expressed on page 62.

$$E_2^o = -4.040 + (8.667 \times 10^{-4})\, T(^oK) \quad \text{(kcal/mole)}$$

and

$$E_3^o = 2E_h + E' - 2.24 \text{(kcal/mole)}$$

or

$$E_3^o = -13.496 + (1.735 \times 10^{-3})\, T(^oK) \quad \text{(kcal/mole)}.$$

The use of these empirically developed cluster potential energies will enable one to extend the cluster concentration distribution to temperatures below 0^oC. The general expression, E_g^o, will allow one to solve for an approximate solution to the equilibrium distribution of clusters of any size if a suitable model for clustering can be found.

CHAPTER IV

VAPOR PHASE CLUSTERING MODEL

A vapor phase clustering model is developed using pentagonal rings of water molecules which are hydrogen bonded with the five oxygen atoms lying in a plane. The rings extend in six directions from a single molecule and result in a three-dimensional network with each ring forming a common interface between adjacent dodecahedral cages. The structure possesses a high degree of symmetry and a large number of hydrogen bonds per molecule with small angular distortion of the free molecular (H-O-H) angle. The unimolecular growth of clusters is determined through the use of the maximization of the number of hydrogen bonds and the requirement that the symmetry be a maximum with minimum distortion of the hydrogen bonds.

This vapor phase clustering model possesses characteristics which provide possible explanations for several physical properties of interfacial or surface liquid water. The clusters contain a continuous distribution of hydrogen bonds which have various degrees of distortion as are probably present in liquid water. The density and structure of the clustering model is similar in several respects to the model which has been proposed for bulk liquid water by Pauling.[53] We have attempted to establish a set of empirical parameters describing the interaction of water molecules in

various states of hydrogen bonding which can be applied in a consistent fashion to the theoretical description of water in all three phases.

IV-1. Description of Model. One of the critical phases of the determination of the equilibrium concentration distribution of clusters is the development of a satisfactory clustering model in the vapor phase. There are many possible configurations for a particular g-cluster, and the only way the problem of calculating the system partition function can be tractable is if there are only a few configurations having a probability of occurence which is much larger than other configurations. The hydrogen bonding of water molecules provides the simplifying condition that there are a limited number of geometrical configurations which need to be considered. Also, the results of the preceding chapter indicate a positive contribution to the cluster potential energy for second nearest neighbors in a hydrogen bonded network, so that an additional constraint on the model of clustering is that the number of second nearest neighbors be a minimum.

A model has been developed utilizing pentagonal rings of water molecules which are hydrogen bonded with the five oxygen atoms in one plane. Starting with an initial water molecule the rings extend in six directions (see Figure 18), and in the resulting three-dimensional network each ring forms a common interface between dodecahedral cages. These cages

have five-fold symmetry which is incompatible with the formation of a crystal lattice, and thus the structure can be extended in three dimensions only to a very limited degree. Extension of the clusters results in unavoidable stress and distortional strain.

The planar pentagonal rings introduce very little distortional strain in the hydrogen bonds as the pentagonal angle of 108° differs only slightly from the tetrahedral coordination angle of 109.5° or the (H-O-H) angle of the free water molecule. Several semiempirical potentials for the (O-H...O) bonding scheme lead to the result that the hydrogen bonds will tend to accommodate themselves to keep the covalent (O-H-O) bond angles close to the equilibrium value of the free molecule.[86-88] Hydrogen bonds in crystals often show large deviations from linearity because of other stabilizing influences of the crystal structure.[91]

Growth of this structure proceeds uniquely in six directions from an initial water molecule to form a network containing dodecahedral holes or cavities, each separated from its twelve somewhat distorted neighboring cavities by twelve planar interfaces of very slightly stressed pentagonal rings. The structure possesses a high degree of symmetry and a large number of hydrogen bonds per molecule with small angular distortion of the free molecular (H-O-H) angle.

An important property of the model is its five-fold symmetry. The interior dihedral angle of the pentagonal

dodecahedron is 116.6°, nearly, but not quite, the 120° angle that would permit the object to fill space solidly. If one regular dodecahedron is attached on each face to twelve other dodecahedra without distortion, none in the outer shell can touch any of its five neighbors. By radial compression and tangential tension, these neighbors may meet and the tangential tension in the peripheral bonds may not be excessive for the first shell. The hydrogen bond is the factor which would permit the growth in size of the clusters by attachment of adjacent dodecahedra, but the distortions of the interior hydrogen bonds would cause breaking and reforming of bonds after the cluster reaches a particular critical size. This is exactly the sort of behaviour demonstrated by liquid water in that one has what appears to be a continuous structure containing a distribution of hydrogen bonds with various amounts of distortion.

Figures 12, 13, 14, and 15 are useful in visualizing the arrangement of water molecules in the proposed vapor clustering model. With dimensions based on the average nearest neighbor distance, 2.90 Å, as used in the dimer and trimer energy calculations, an element or cage can be inscribed in a sphere of 8.15 Å diameter, and a sphere of 6.34 Å diameter can be inscribed inside a cage. Only a central cage of a cluster can be truly symmetrical. The surrounding dodecahedra have to be distorted in order to connect with their neighbors.

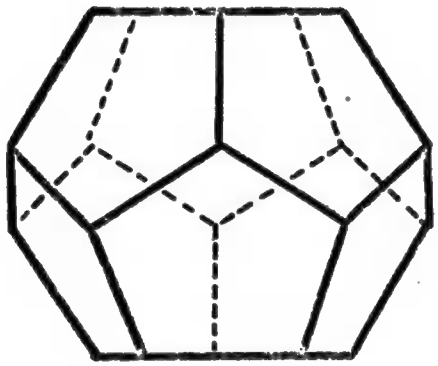

Figure 12. Side View of Pentagonal Dodecahedron.

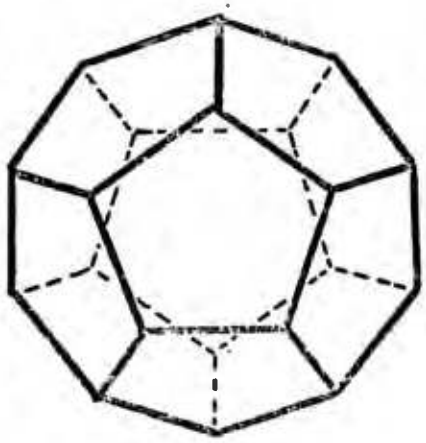

Figure 13. Top View of Pentagonal Dodecahedron.

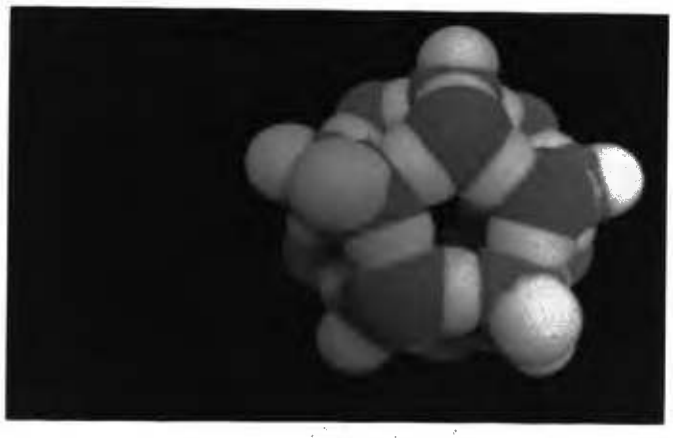

Figure 14. Dodecahedral Cluster of Twenty Water Molecules. The van der Waals' Radii are used to Properly Represent the Size of the Cavity.

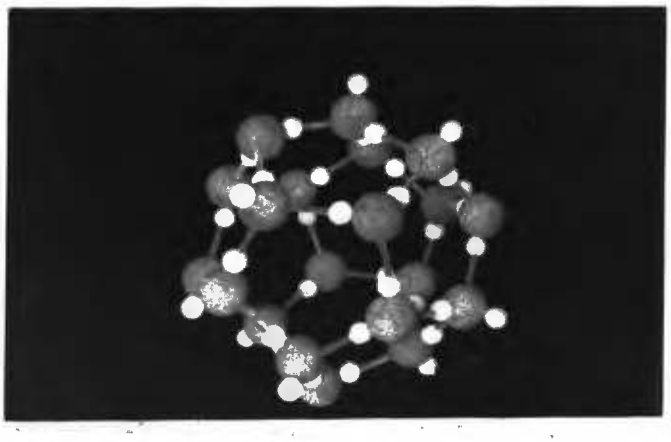

Figure 15. Dodecahedral Cluster of Water Molecules with Smaller Radii for the Atoms to Show the Structure.

In order to obtain an estimate of the density of the clusters, the distortion is neglected and unlimited continuity is assumed. There would be five water molecules per dodecahedral unit (20 molecules in the dodecahedron with each shared by 4 dodecahedra), and the density is computed from the molecular weight of water and the cage dimensions as

$$d_o = 5m/V = \{5\}(18.015)/(6.0225\times10^{23})(7.6631)(2.9\times10^{-8})^3$$

or

$$d_o = 0.80 \text{ gm cm}^{-3} \quad .$$

If one, two, or three molecules are able to be distributed to each of the interior cavities of the various dodecahedra, the resulting densities are, respectively,

$$d_1 = 0.96 \text{ gm cm}^{-3}$$
$$d_2 = 1.12 \text{ gm cm}^{-3}$$
$$d_3 = 1.28 \text{ gm cm}^{-3}.$$

These values of density are certainly compatible with the observed liquid water density.

The continuity assumed above cannot exist indefinitely when the liquid is cooled below the freezing point, because of the five-fold symmetry and the inherent distortions of the clusters. The very existence of this five-fold symmetry does, however, provide an explanation for the ability of liquid droplets to form in the vapor phase below the normal freezing point.

A recent article by Horne[93] indicates properties of interfacial water which seem to support the possibility that the structure of surface water may be similar to the structure postulated in this work. The general problem of interfacial water could be attacked with the techniques used in the present study, and extensive calculations might determine the structure.

If the vapor phase clustering model as developed here is correct, the interfacial water between the bulk liquid and the vapor phase would be expected to be similar in nature to the cluster structure because this would be the most stable form. The water surface would appear to be the concave and convex surfaces of the dodecahedral cages. Each of the surface molecules would be participating in three or four distorted hydrogen bonds explaining the relatively low vapor pressure at temperatures near 0°C. As the temperature is increased, further distortion of the bonds occurs to weaken the bonds enabling more of the surface molecules to escape to the vapor phase.

The primary concern in the present work is to determine how the unimolecular growth occurs in the vapor phase clusters, so that the most stable clusters may be used in the calculation of the partition function of the system of clusters of various sizes. This growth process is discussed in the next section.

IV-2. Unimolecular Growth of Clusters. An important consideration is the actual configuration of a particular g-cluster. In this section, the growth process is postulated through the use of the maximization of the number of bonds and requiring the maximum symmetry with minimum distortion or bending of the hydrogen bonds. The results of the calculation of the second neighbor contribution to the cluster energy indicate that a critical condition is that the number of second nearest neighbors should be minimized. Cluster models containing various numbers of molecules have been constructed in this development. The dimer and trimer are indicated in Figure 9, while various other clusters are pictured in Figures 14 through 18.

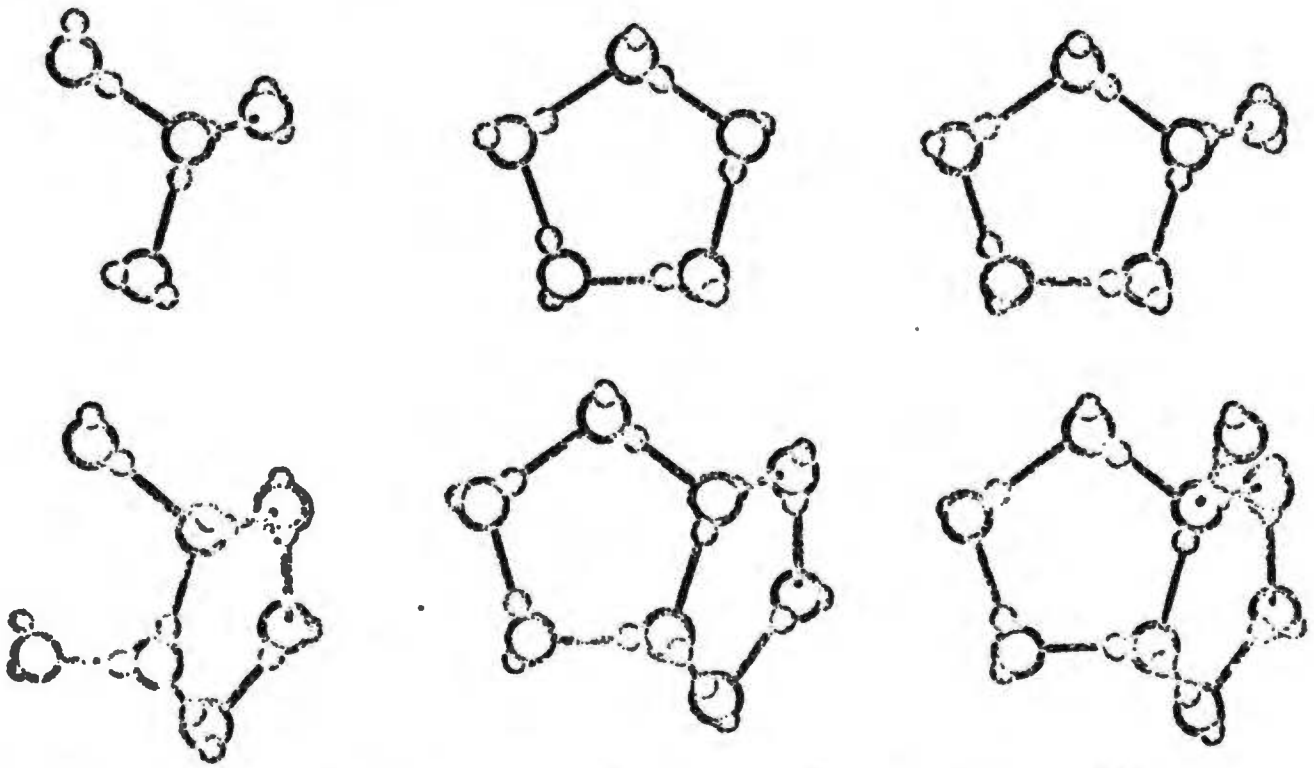

Figure 16. Water Clusters Containing Four, Five, Six, Seven, Eight, and Nine Molecules.

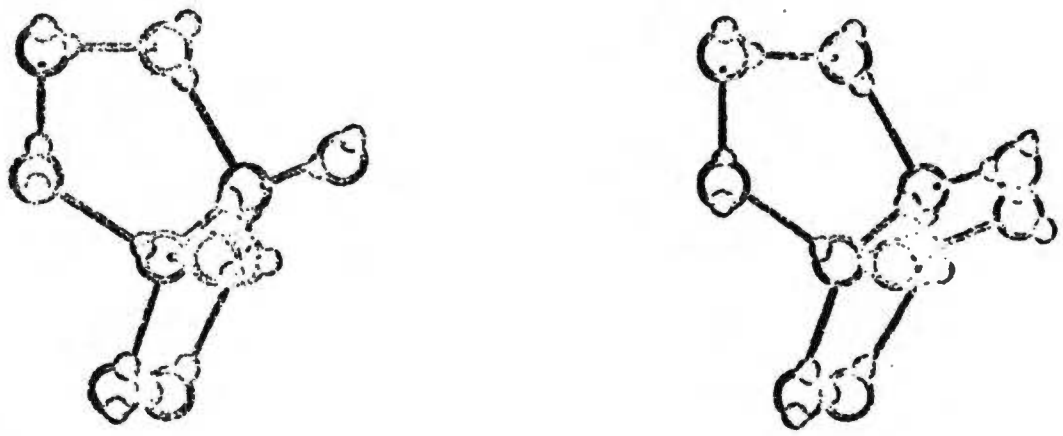

Figure 17. Water Clusters Containing Ten and Eleven Molecules.

As an example of the procedure in selecting the proper cluster model, consider a cluster containing five molecules. The plane pentagonal ring contains five hydrogen bonds while the tetrahedral cluster of Figure 6 has four hydrogen bonds. In addition, the pentagonal ring has five second nearest neighbor interactions while the tetrahedral cluster has six. Therefore, the pentagonal ring is the most favorable under both conditions. The various sizes of cluster can be built up in the manner indicated as far as one needs to go. Figure 19 shows clusters containing seventeen, fifty-seven, and seventy molecules, respectively. An interesting point is that bowls or half completed cavities are formed during the growth process, and these would seem to be capable of trapping a molecule of the noncondensible gas. The cluster might then grow around the trapped gaseous molecule, enclosing it in a dodecahedral cage.

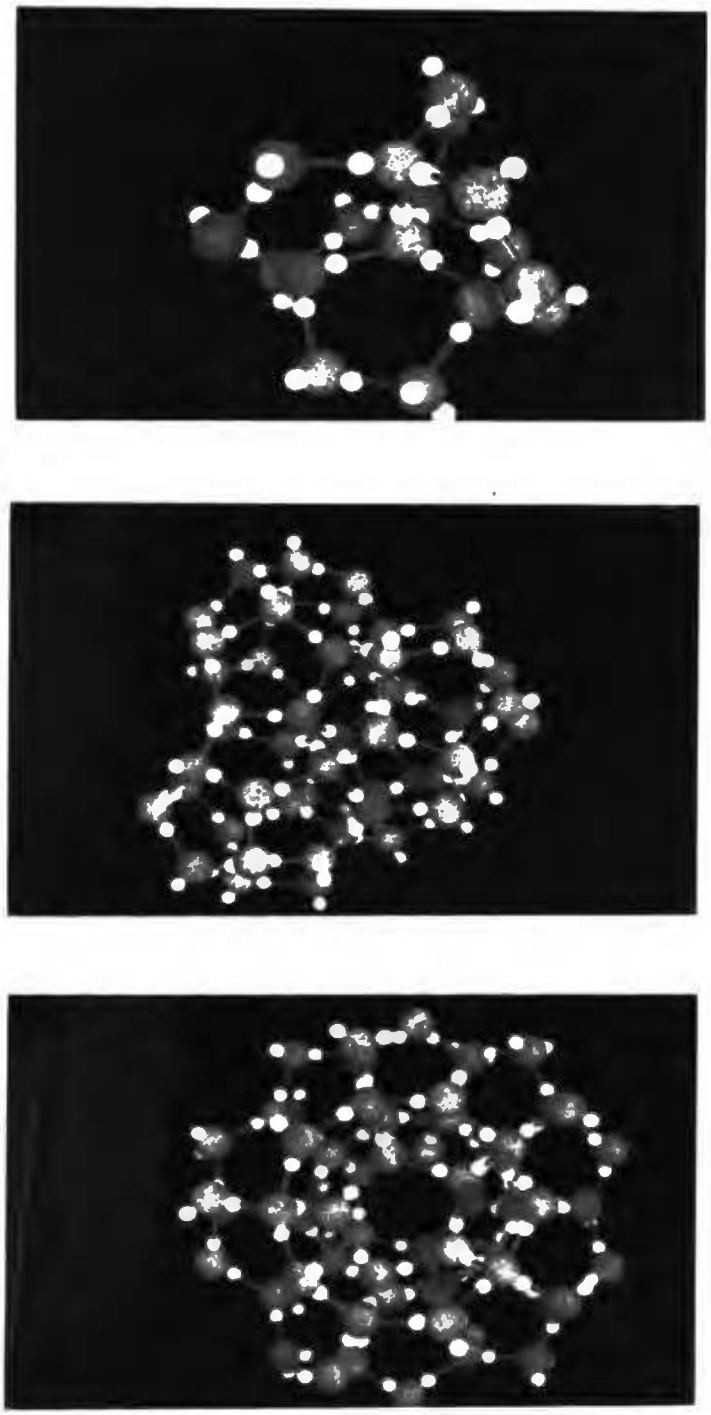

Figure 18. Water Clusters Containing Seventeen, Fifty-seven, and Seventy Molecules, Respectively.

CHAPTER V

SUMMARY AND DISCUSSION

V -1. Summary of Results. Several important conclusions can be drawn from this study of how one may determine the equilibrium concentration of clusters of water molecules in the vapor. The following is a summary of the results of this work with comments on the validity of various assumptions used in the calculations.

A simple semiempirical method is developed for determining the hydrogen bond energy in dimers and trimers of water in the vapor phase. The technique is based on a general statistical mechanical theory of clustering in which the partition function for a system of non-interacting clusters is used in conjunction with empirical values of the concentration equilibrium constants of the dimer and trimer. Estimated values of the stretching and bending force constants are based on values reported in the literature on infrared and Raman spectral studies. The results for the dimer agree quite well with quantum mechanical calculations. The general expression for the g-cluster interaction potential energy is expressed as

$$E_g^o = \alpha E_h + \beta E' + E_g^{d-d}$$

where

$$E_h = -4.788 + (8.667\times10^{-4})\,T \qquad \text{(kcal/mole)}$$

and

$$E' = -1.680 + (1.640\times10^{-2})\,T \qquad \text{(kcal/mole)},$$

and α is the number of nearest neighbors; β, the number of second nearest neighbors; and E_g^{d-d}, the total dipole-dipole interaction energy of the g-cluster.

The results that the nearest hydrogen bonded neighbor energy is negative and the second nearest neighbor energy is positive provide a means of selecting the probable structures for the clusters in the vapor. To minimize the potential energy, the number of hydrogen bonds in the cluster should be a maximum. If two cluster structures have the same number of hydrogen bonds, the cluster with the smaller number of second nearest neighbor interactions would be the preferable form.

The cluster model thus developed is made up of pentagonal rings of water molecules which are hydrogen bonded into a network of pentagonal dodecahedral cages. These cages have five-fold symmetry which is incompatible with the formation of a crystal lattice, explaining the ability of liquid droplets to nucleate at temperatures below the normal freezing point.

These results are compatible with the known properties of liquid water as outlined in Chapter II. Various workers have demonstrated that solid state-like oscillations of the water molecules in liquid water are present and this suggests the presence of firmly bonded aggregates.[86] Indeed, the model does provide a continuum structure with varying degrees of distortion of the hydrogen bonds.

V -2. Sources of Errors. Many criticisms can be made of several of the developments and calculations in this study. The major problem, however, is how to overcome these difficulties. The following is a summary of some of the more important weaknesses of the present work.

The first point of interest is in the development of the statistical thermodynamic expression for the concentration equilibrium constants. The interactions between clusters have been completely ignored. This does eliminate the problem of attempting to develop an expression for the interaction potential between clusters, and Reiss[87] has pointed out that this is a good approximation as long as the system is far away from the critical temperature and pressure. Under these conditions, the actual physical clusters with which this work is concerned correspond directly to the mathematical clusters in the cell model presented by Reiss.[88] The neglect of the cluster-cluster interactions should be appropriate in the vapor under the cloud chamber conditions, but major difficulties are introduced if one attempts to extend the approach to the bulk liquid phase.

The reliability of the values of the estimated force constants for distorting the hydrogen bonds are questionable on several grounds. The geometry and effective force constants for an isolated water molecule are well known,[89] but seemingly unsurmountable difficulties arise in attempting to determine force constants in a crystalline structure

such as ice. There is evidence that the molecular bond angle may be 105° as it is in the isolated molecule, and there may be some further disorder around the (O...O) lines.[90] Hamilton and Ibers[91] have pointed out that evidence from infrared and Raman spectra suggest that a variety of (O...O) distances exist in the ice structure, and each of these different bond lengths will have associated with them a different force constant, hence a different frequency. In any case, it is not possible to account for the spectra of ice and to determine force constants because of the many factors complicating the situation. In a crystalline solid, vibrations occur such that molecules or molecular groups are oscillating relative to other similar groups making it extremely difficult to identify exactly what the source of a particular vibrational frequency might be. The actual potential energies are not symmetrical and the frequencies are amplitude dependent. The librational potential energy is coupled to the stretching frequencies through the amplitude of the stretching oscillations. Since all of these complications enter, one might wonder whether the calculations in this work have any validity whatsoever.

In order to justity the technique used, one must look at previous work in clustering phenomena. A standard approach is to assume that the (9g - 6) internal degrees of freedom are all completely energy activated so that the total energy contribution due to the internal degrees of freedom is

equal to (9g - 6)kT/2 for a g-cluster. This sort of assumption is not at all realistic for the water clusters because the complete excitation of a single vibrational state at the temperatures of interest would be sufficient to break up the cluster. This particular assumption has met with fair success in the clustering of monatomic gases at low temperatures. In the case of water near $0^{\circ}C$, any mode with a characteristic temperature more than four times the temperature of the system would make only ground state contributions to the energy. The approximate approach used here is an attempt to get closer to reality, and the quantum mechanical calculations indicated in Table VII seem to indicate success in this regard.

Another question arises over the use of the equally spaced energy levels of a simple harmonic potential and performing the summation over all levels, that is, letting N_m approach a very large value in the expression

$$\sum_{n}^{N_m} \exp\ (-E_m^n/kT) \quad .$$

Certainly, only a few states are possible in the actual potential, and they are definitely not equally spaced but approach a continuum of levels as the amplitude of vibration increases. Again, the justification of this approximation must be taken from the agreement with theoretically calculated binding energies for the dimer.

The assumption that the dimer and trimer interaction potentials exclusive of dipole-dipole contributions can be accounted for by a simple linear combination of two single hydrogen bond energies and a single second neighbor interaction energy might be called an oversimplification. There does not seem to be any other way to get around this problem at this time, because there is no simple way available to separate the coupling effect between the two hydrogen bonds from the second neighbor interaction. Earlier calculations in this study were made assuming the hydrogen bond length was nearly the same in vapor clusters as observed in ice and the strength of the hydrogen bonds were related to the number of nearest neighbors via an empirically determined exponent on the number of nearest neighbors. This procedure cannot be used here because the bond lengths are not equal.

The various configurations for a particular g-cluster model are not equally probable as assumed in the development; however, in order to make the problem more tractable, an average dipole-dipole energy is calculated and used in the partition function. Again, this may not be exact, but it seems to be a good first approximation.

To obtain exact results, all possible structures of g-clusters should be considered when calculating the partition function. This is an impossibility, because the interaction potential energy is not known as a function of intermolecular separation and orientation. Since the

probability of bonding in the tetrahedral coordination is large, as evidenced by liquid and solid spectra, use of the hydrogen bonded scheme should give fairly reliable predictions of cluster structure.

The final consideration of this section is the effect of changing various parameters in the expression for K_g, the concentration equilibrium constant,

$$K_g = Q_{gt}Q_{gr}Q_{gi}\exp(-E_g^o/kT) \;/\; V\, g!\; (Q_1/V)^g \quad .$$

The cluster translational contributions, Q_{gt}, and the monomer partition function, Q_1, are known accurately. The questionable contributions are the cluster rotational, Q_{gr}, and the cluster internal, Q_{gi}, contributions as well as the cluster binding energy, E_g^o. That is to say, one needs to consider effects of errors in these quantities.

$$K_g \approx C\,(A_gB_gC_g)^{\frac{1}{2}}\, r_g \prod_m f_{gm} \exp(-E_g^o/kT) \;/\; \sigma_g \prod_s X_s!$$

All of these quantities are strongly model dependent so that the cluster structure is of prime importance. The agreement of the dimer calculations with other work supports the linear bond concept, so that this probably is a satisfactory assumption in larger clusters.

The fractional variation in K_g may be approximated by considering the differential of the $\ln(K_g)$, resulting in the observation that, in all cases except the cluster potential energy, E_g^o, errors in the various parameters will result in

comparable percentage errors in K_1. The critical term is the cluster potential energy, E_g^o, because the percentage error in K_g is proportional to the error in E_g^o. This means the value of E_g^o as calculated for the dimer and trimer is fairly reliable, because a 10% error in the empirical value of K_2 would result in an error of 0.05 kcal/mole in E_2^o if the other parameters are held fixed. On the other hand, at 0°C, an error of 100% in K_g would result from an error of 0.54 kcal/mole in the estimated value of E_g^o. This points out the importance of having an extremely accurate determination of the dependence of E_g^o on the temperature and the structure. Until the calculations are extended to larger clusters and the nucleation rate determined, the reliability of the cluster potential energies cannot be tested experimentally.

V -3. Suggestions for Further Work. As more time is devoted to this study, it seems that the actual end of the development recedes further into the future. A molecular approach is definitely necessary in nucleation theory, but there are not any guide posts along the route of the development. One must travel the path in the dark with only distant reference points available such as knowledge of the properties of liquid water and ice.

The current path should be pursued until results are obtained for the equilibrium concentration of g-clusters based

on the dodecahedral clustering model. This would enable the calculation of the nucleation rate for homogeneous nucleation in pure water vapor. An attempt could then be made to incorporate the non-condensible gas and hydrogen peroxide into the clustering process to test the theory with actual cloud chamber observations.

The next step would be to develop the theory on the basis of a more realistic molecular interaction potential than the simple harmonic potential. This will be extremely difficult, but with the experience gained from the initial development, it should be possible. The Morse potential would probably be best for this second development. A method for determining normal modes of vibration would be to construct actual physical clusters of springs and metal spheres. The basic problem with this approach is, again, the actual force contants of the real clusters cannot be represented by a simple spring. It would be impossible to construct springs with the proper angular variations and asymmetric stretching characteristics even if the proper characteristics were known.

The current plan is to continue the work with the larger clusters assuming the expressions obtained for E_h and E' are accurate with the hope that satisfactory agreement with the experimental observations can be attained.

APPENDIX I
ESTIMATE OF TRIMER VIBRATION FREQUENCIES

The set of equations on page 52 for the internal vibrational motion of the trimer is solved in this appendix. The angle α_o is assumed to be 109^o, so that the set of equations becomes

$$m\ddot{x}_1 + k_r(x_1 + 0.5807\, x_2 + 0.5807\, y_2) = 0$$
$$m\ddot{x}_2 + k_r(0.5807\, x_1 + x_2 - 0.8141\, x_3) = 0$$
$$m\ddot{y}_2 + k_r(0.5807\, x_1 - 0.3256\, x_2 + 0.8141\, x_3) = 0$$
$$m\ddot{x}_3 + k_r(-0.8141\, x_2 + 0.8141\, y_2 + x_3) = 0$$
$$m\ddot{\theta}_1 + k_\theta(\theta_1 - \theta_{21}) = 0$$
$$m\ddot{\theta}_{21} - k_\theta(\theta_1 - \theta_{21}) = 0$$
$$m\ddot{\theta}_{22} + k_\theta(\theta_{22} - \theta_3) = 0$$
$$m\ddot{\theta}_3 - k_\theta(\theta_{22} - \theta_3) = 0$$

The last four equations are independent of the first four with the approximations that have been made in the development presented in the text. In fact, we have three sets of independent equations which may be written as

$$\omega_r^{-2}\ddot{x}_1 + x_1 + 0.5807\, x_2 + 0.5807\, y_2 = 0$$
$$\omega_r^{-2}\ddot{x}_2 + 0.5807\, x_1 + x_2 - 0.8141\, x_3 = 0$$
$$\omega_r^{-2}\ddot{y}_2 + 0.5807\, x_1 - 0.3256\, x_2 + y_2 + 0.8141\, x_3 = 0$$
$$\omega_r^{-2}\ddot{x}_3 - 0.8141\, x_2 + 0.8141\, y_2 + x_3 = 0 \quad ,$$

$$\omega_\theta^{-2}\ddot{\theta}_1 + \theta_1 - \theta_{21} = 0$$
$$\omega_\theta^{-2}\ddot{\theta}_{21} - \theta_1 + \theta_{21} = 0 \quad ,$$

$$\omega_\theta^{-2}\ddot{\theta}_{22} + \theta_{22} - \theta_3 = 0$$
$$\omega_\theta^{-2}\ddot{\theta}_3 - \theta_{22} + \theta_3 = 0 \quad ,$$

where $\omega_r = (k_r/m)^{1/2}$ and $\omega_\theta = (k_\theta/m)^{1/2}$.

A set of homogeneous second-order differential equations

$$\ddot{x}_i + \sum_j b_{ij}x_j = 0 \qquad (i = 1,\ldots,N)$$

is known always to possess solutions of the form

$$x_i = x_i^o \exp(j\omega t) \qquad (i = 1,\ldots,N)$$

where x_i^o and ω are constants. These solutions are now substituted into the above equations in order to evaluate the constants. The substitution yields

$$(1 - \omega^2/\omega_r^2)\, x_1^o + 0.5807\, x_2^o + 0.5807\, y_2^o = 0$$
$$0.5807\, x_1^o + (1 - \omega^2/\omega_r^2)\, x_2^o - 0.8141\, x_3^o = 0$$
$$0.5807\, x_1^o - 0.3256\, x_2^o + (1 - \omega^2/\omega_r^2)\, y_2^o + 0.8141\, x_3^o = 0$$
$$-0.8141\, x_2^o + 0.8141\, y_2^o + (1 - \omega^2/\omega_r^2)\, x_3^o = 0 \quad ,$$

$$(1 - \omega^2/\omega_\theta^2)\, \theta_1^o - \theta_{21}^o = 0$$
$$-\theta_1^o + (1 - \omega^2/\omega_\theta^2)\, \theta_{21}^o = 0 \quad ,$$

$$(1 - \omega^2/\omega_\theta^2)\, \theta_{22}^o - \theta_3^o = 0$$
$$-\theta_{22}^o + (1 - \omega^2/\omega_\theta^2)\, \theta_3^o = 0 \quad .$$

These simultaneous equations only have solutions other than the trivial ones $x_1^o = x_2^o = \ldots = x_3^o = 0$ if the determinant formed from the coefficients of the x_i^o's vanishes.

$$\begin{vmatrix} (1 - \omega^2/\omega_r^2) & 0.5807 & 0.5807 & 0 \\ 0.5807 & (1 - \omega^2/\omega_r^2) & 0 & -0.8141 \\ 0.5807 & -0.3256 & (1 - \omega^2/\omega_r^2) & 0.8141 \\ 0 & -0.8141 & 0.8141 & (1 - \omega^2/\omega_r^2) \end{vmatrix} = 0$$

$$\begin{vmatrix} (1 - \omega^2/\omega_\theta^2) & -1 \\ -1 & (1 - \omega^2/\omega_\theta^2) \end{vmatrix} = 0$$

$$\begin{vmatrix} (1 - \omega^2/\omega_\theta^2) & -1 \\ -1 & (1 - \omega^2/\omega_\theta^2) \end{vmatrix} = 0$$

The last two equations yield the result that $\omega = (2)^{\frac{1}{2}}\omega_\theta$ as was obtained in the case of the dimer. It is assumed that each of the four coordinates has associated with it the vibrational frequency, $\nu = \omega/2\pi$.

Upon expansion of the determinant of the first equation, the fourth order equation in $x(=\omega/\omega_r)$

$$x^4 - 2.0000x^2 + 0.1060x + 0.8940 = 0$$

is obtained. The roots to this equation are 1, 1, -0.755, and -1.22. The two negative roots indicate that we don't have a stable configuration with the potentials as assumed here. However, in order to perform the calculation of the trimer bond energy, it is assumed that the solution, $x = 1$, is valid and the four vibration frequencies are taken to be $\omega = \omega_\theta$.

It is obvious that this determination of the characteristic frequencies is very approximate for several reasons. These sources of error are discussed in Chapter VI of this dissertation. These include the complete neglect of coupling between the various vibrations; however, more basic to this approximation is the fact that the true potential energy is not known.

APPENDIX II
ESTIMATE OF MOMENTS OF INERTIA

The cluster moments of inertia and internal moments of inertia are also model dependent, and depend upon the length of the hydrogen bond. The monomer values of the principle moments of inertia have been determined from microwave spectroscopy[41] and are equal to

$$A_1 = 9.96 \times 10^{-41} \quad \text{gm cm}^2$$
$$B_2 = 1.908 \times 10^{-40}$$
$$C_2 = 2.98. \times 10^{-40}$$

For the dimer, the two moments of inertia about axes perpendicular to the hydrogen bond are calculated by assuming the two molecules to be point masses separated by R(O-H...O), the hydrogen bond length. This yields

$$A_2 = B_2 = 5.97 \times 10^{-40} \; R^2 \qquad (\text{gm cm}^2)$$

where R is in Ångstroms. The moment of inertia about the bond axis is calculated using the observed atomic separation[41] of the O-H bond. For one molecule, the rotation is about one of the (O-H) axes

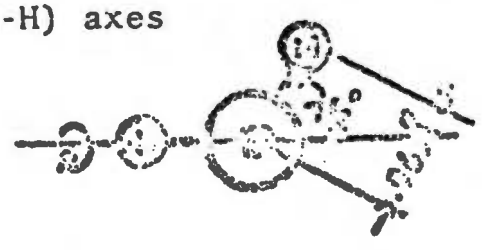

so that the moment of inertia is due to a single hydrogen at a distance of $(0.96 \times \sin 76^{\circ}) = .93$ Å, resulting in a value

of

$$I_1 = 1.44 \times 10^{-40} \quad \text{gm cm}^2.$$

The other molecule is oriented so that the hydrogen bond nearly bisects the HOH angle

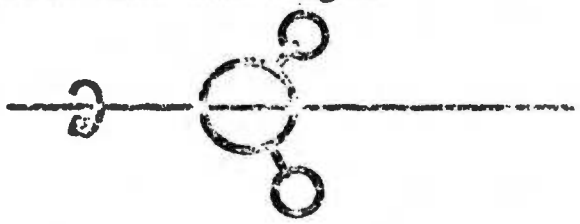

so that the moment of inertia is due to two hydrogens at a distance of .96x sin53° Angstroms from the axis of rotation.

$$I_2 = 1.97 \times 10^{-40} \quad \text{gm cm}^2$$

I_1 and I_2 correspond to the internal moments of inertia for rotation about the single bond, and their sum is the value of C_2,

$$C_2 = 3.41 \times 10^{-40} \quad \text{gm cm}^2 \quad .$$

In the trimer, the molecules are again considered as point masses in the calculation of the cluster moment of inertia. The values obtained are

$$A_3 = 3.07 \times 10^{-39} \quad \text{gm cm}^2$$
$$B_3 = 3.82 \times 10^{-39}$$
$$C_3 = 5.45 \times 10^{-40} \quad .$$

The internal rotations include two at the values of I_1 and I_2 which average to 1.50×10^{-40} gm cm^2 and two with the rotation of a molecule about the hydrogen bond in which it is not

participating,

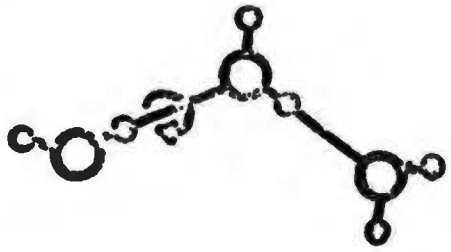

This yields

$$I_3 = 1.53 \times 10^{-38} \quad \text{gm cm}^2$$

APPENDIX III
ESTIMATE OF DIPOLE-DIPOLE INTERACTION ENERGIES

In order to estimate the cluster interaction potential accurately, it is best to separate as many known contributions as possible. The net dipole-dipole energy is one contribution that can be removed if the cluster structure is known.

Because of the rotation about the single bond in the dimer, the dimer dipole-dipole contribution can be pictured as the interaction between two dipoles $\mu_1 (= \mu\cos 71^\circ)$ and $\mu_2 (= \mu\cos 54.5^\circ)$ which are in the same direction along the hydrogen bond axis and separated by R = 2.90 Å.

or

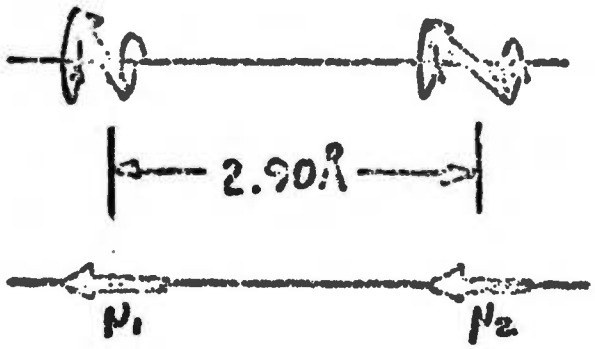

The general expression for the dipole-dipole energy is[94]

$$E = \mu_1\mu_2 R^{-3}(2 \cos\theta_1 \cos\theta_2 - \sin\theta_1 \sin\theta_2 \cos(\phi_2 - \phi_1)).$$

In the case of the dimer, $\theta_1 = \theta_2 = \phi_1 = \phi_2 = 0$, because of the rotation about the single bond. For water, $\mu = 1.83\times10^{-18}$ e.s.u.,[94] resulting in a dipole-dipole energy of

$$E_2^{d-d} = -0.748 \text{ kcal/mole} \quad .$$

In the trimer, we have the three configurations indicated in Figure 9. The dipole-dipole interaction energy is calculated for each configuration and then averaged to obtain the effective trimer dipole-dipole term. In type I,

the rotations about the two bonds give us the effective configuration

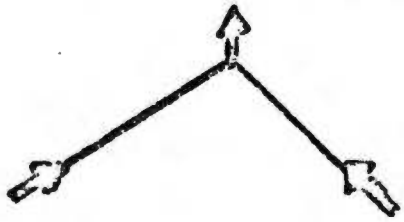

so that the interaction between molecules 1 and 2 and that between 2 and 3 are

$$- \mu^2 \cos 54.5^\circ \, R^{-3} \, (2 \cos 54.5^\circ) \quad .$$

The dipole-dipole energy between 1 and 3 is

$$\mu^2 \cos^2 54.5^\circ \, (2 R \cos 35.5^\circ)^{-3} (2 \cos^2 35.5^\circ - \sin^2 35.5) .$$

The net dipole-dipole energy of the type I trimer is

$$E_3^{oI} = - 2.515 \text{ kcal/mole} \quad .$$

Similar calculations for types II and III

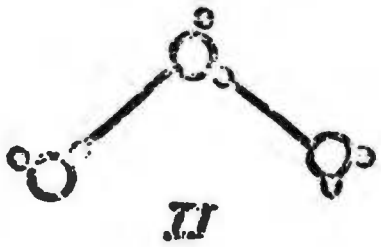

II

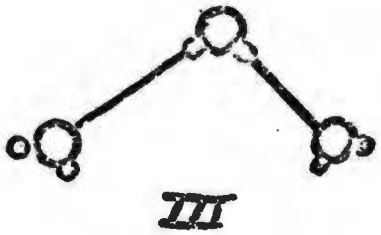

III

yield

$$E_3^{oII} = -1.582 \quad \text{kcal/mole}$$

and

$$E_3^{oIII} = -2.620 \quad \text{kcal/mole} \ .$$

The average of these three values is

$$E_3^{o} = -2.239 \quad \text{kcal/mole.}$$

BIBLIOGRAPHY

1. B. J. Mason, The Physics of Clouds, Oxford Press, (1957).
2. L. Allen, An Experimental Determination of the Homogeneous Nucleation Rate of Water Vapor in Argon and Helium, Dissertation, University of Missouri - Rolla, (1968).
3. F.P. Parungo and J. P. Lodge, Jr., J. Atm. Sci. 24, 439, (1967).
4. C. T. R. Wilson, Proc. Camb. Phil. Soc. 8, 306, (1895).
5. J. W. Gibbs, The Collected Works of J. Willard Gibbs, Vol. I, Longmans Press, (1928).
6. M. Volmer and A. Weber, Z. physik Chem. A119, 277, (1926).
7. L. Farkas, Z. Physik Chem. A125, 236, (1927).
8. M. Volmer, Z. Electrochem. 35, 555, (1929).
9. R. Kaischew and I. N. Stranski, Z. physik Chem. B26, 317, (1934).
10. R. Becker and W. Doring, Ann. physik 24, 719, (1935).
11. M. Volmer, Kinetik der Phasenbildung, Dresden, (1939).
12. J. Frenkel, Kinetic Theory of Liquids, Oxford Press, (1946).
13. A. Bijl, Discontinuities in the Energy and Specific Heat, Leiden, (1938).
14. D. Turnbull and J. H. Hollomon, The Physics of Powder Metallurgy, edited by W. E. Kingston, McGraw-Hill, (1951).
15. R. S. Bradley, Quarterly Rev. (London) 5, 315, (1951).
16. V. K. LaMer, Ind. Engr. Chem. 44, 1270, (1952).
17. G. M. Pound, Ind. Engr. Chem. 44, 1278, (1952).
18. D. Turnbull, Solid State Physics, Academic Press, (1956).
19. W. G. Courtney, J. Chem. Phys. 36, 2018, (1962).
20. F. F. Abraham and G. M. Pound, J. Chem. Phys. 48, 732, (1968).
21. H. Reiss, J. L. Katz, and E. R. Cohen, J. Chem. Phys. 48, 5553, (1968).

22. W. G. Courtney, J. Phys. Chem. 72, 421, (1968).

23. J. Lothe and G. M. Pound, J. Chem. Phys. 36, 2080,(1962).

24. J. Feder, J. P. Hirth, J. Lothe, K. C. Russell, and G. M. Pound, Prog. Astron. Aeron. 15, 667, (1964).

25. J. Feder, K. C. Russell, J. Lothe, and G. M. Pound, Adv. Phys. 15, 111, (1966).

26. J. P. Hirth, Ann. N. Y. Acad. Sci. 101, 805, (1963).

27. R. A. Oriani and B. E. Sundquist, J. Chem. Phys. 38, 2082, (1963).

28. F. Kuhrt, Z. Physik. 131, 205, (1952).

29. W. J. Dunning, Proceedings of the Case Institute of Technology Symposium on Nucleation, Cleveland, (1965).

30. J. Zeldovich, J. Exp. Theor. Phys. (Russian) 12, 525, (1942).

31. C. N. Yang and T. D. Lee, Phys. Rev. 87, 404, (1952).

32. R. C. Tolman, J. Chem. Phys. 17, 335, (1949).

33. F. P. Buff, J. Chem. Phys. 17, 338, (1949).

34. F. P. Buff, J. Chem. Phys. 23, 419, (1955).

35. J. W. Cahn and J. E. Hilliard, J. Chem. Phys. 28, 258, (1958).

36. H. Reiss, J. Chem. Phys. 20, 1216 (1952).

37. E. W. Hart, Phys. Rev. 113, 412, (1959).

38. J. W. Cahn, J. Chem. Phys. 30, 1121, (1959).

39. E. R. Buckle, A Theory of Condensation and Evaporation of Aerosols, U. S. Naval Acadamy, (1966).

40. H. M. Chadwell, Chem. Rev. 4, 375, (1927).

41. G. C. Pimentel and A. L. McClellan, The Hydrogen Bond, W. H. Freeman Co., (1960).

42. M. Falk and T. A. Ford, Can. J. Chem. 44, 1699, (1966).

43. G. Oster and J. G. Kirkwood, J. Chem. Phys. 11, 175, (1943).

44. J. A. Pople, Proc. Roy. Soc. (London), 205A, 163, (1951).

45. F. E. Harris and B. J. Alder, J. Chem. Phys. 21, 1351, (1953).

46. G. N. Haggis, J. B. Hasted, and T. J. Buchanan, J. Chem. Phys. 20, 1452, (1952).

47. G. Nemethy and H. A. Scheraga, J. Chem. Phys. 36, 3382, (1962).

48. H. S. Frank and W. Y. Wen, Disc. Far. Soc. 24, 133, (1957).

49. J. Morgan and B. E. Warren, J. Chem. Phys. 6, 666, (1938).

50. M. Danford and H. Levy. J. Am. Chem. Soc. 84, 3965, (1962).

51. P. C. Cross, J. Burnham. and P. A. Leighton, J. Am. Chem. Soc. 59, 1134, (1937).

52. G. E. Walrafen, J. Chem. Phys. 40, 3249, (1964).

53. L. Pauling, Hydrogen Bonding, edited by Hadzi, Pergamon, (1959).

54. L. Pauling, The Nature of the Chemical Bond, Cornell, (1960).

55. M. von Stackelberg, Fortschr. Mineral 26, 122, (1947).

56. M. von Stackelberg, J. Chem. Phys. 19, 1319, (1951).

57. W. S. Claussen, J. Chem. Phys. 19, 259, 662, 1425, (1951).

58. H. A. Levy, Chem. Div. Ann. Prog. Rept., May 20, 1966, ORNL-1940, p. 129.

59. J. B. Hasted, private communication.

60. J. D. Bernal and R. H. Fowler, J. Chem. Phys. 1, 575, (1933).

61. R. P. Marchi and H. J. Eyring, J. Phys. Chem. 68, 221, (1964).

62. H. S. Frank, Proc. Roy. Soc. (London) A247, 481, (1958).

63. L. Hall, Phys. Rev. 73, 775, (1948).

64. M. Falk and T. A. Ford, Can. J. Chem. 44, 1699, (1966).

65. H. Yamatera, B. Fitzpatric, and G. Gordon, J. Mol. Spect. 14, 263, (1964).

66. M. J. Sparnaay, J. Coll. Interface Sci. 22, 23, (1966).

67. a) B. V. Deragin, et.al., Dokl. Akad. Nauk. SSSR 170, 876, (1966).
b) B. V. Deragin, et.al., Disc. Far. Soc. 42, 109, (1966).
c) B. V. Deragin, et.al., Isv. Akad. Nauk. SSSR, Ser. khim, 10, 2178, (1967).

68. a) P. G. Owston, J. chim. phys. 50, C13, (1953).
b) P. G. Owston, Quart. Revs. (London) 5, 344, (1951).
c) P. G. Owston, Adv. in Phys. 7, 171, (1958).

69. N. Bjerrum, Kgl. Danske Videnskab. Selskab., Mat.-fys. Medd. 27, No. 1, (1951).

70. K. Lonsdale, Proc. Roy. Soc. 247A, 424, (1958).

71. J. E. Bertie and E. Whalley, J. Chem. Phys. 46, 1271, (1967).

72. P. A. Giguere and J. P. Arraudeu, Compt Rend. 257, 1692, (1963).

73. F. G. Keyes, J. Chem. Phys. 15, 602, (1947).

74. W. Band, An Introduction to Quantum Statistics, D. Van Nostrand Co., (1955).

75. O. Glemser and E. Hartert, Z. anorg. u allgem. Chem. 283, 111, (1956).

76. J. Karle and L. O. Brockway, J. Am. Chem. Soc. 66, 574, (1944).

77. F. Holtzberg, B. Post, and I. Fankuchen, Acta. Cryst. 6, 127, (1953).

78. R. E. Jones and O. H. Templeton, Acta. Cryst. 11, 484, (1958).

79. C. A. Coulson and V. Danielsson, Arkiv. for Fysik. 8, 245, (1954).

80. P. C. McKinney and G. M. Barrow, J. Chem. Phys. 31, 294, (1959).

81. R. Grahn, Arkiv. for Fysik 15, 257, (1959).

82. J. S. Rowlinson, Tran. Far. Soc. 45, 974, (1949).

83. C. A. Coulson, Research (London) 10, 149, (1957).

84. K. Morokuma and L. Pedersen, J. Chem. Phys. 48, 3275, (1968).

85. R. T. Hall and J. M. Dowling, J. Chem. Phys. 47, 2454, (1967).

86. A. Rahman, K. Singwi, and A. Sjolander, Phys. Rev. 126, 986, (1952).

87. H. Reiss, private communication.

88. H. Reiss, Ind. Eng. Chem. 44, 1284, (1952).

89. D. F. Heath and J. W. Linnett, Trans. Far. Soc. 44, 556, (1948).

90. R. Chidambaram, Acta Cryst. 14, 467, (1961).

91. W. C. Hamilton and J. A. Ibers, Hydrogen Bonding in Solids, W. A. Benjamin, Inc., (1968).

92. H. W. Woolley, J. Chem. Phys. 21, 236, (1953).

93. R. A. Horne, A. F. Day, R. P. Young, and N. T. Yu, Electrochim. Acta, 13, 397, (1968).

94. J. O. Hirschfelder, C. F. Curtiss, and R. B. Bird, Molecular Theory of Gases and Liquids, Wiley, New York, (1954).

95. W. J. Eadie, A Molecular Theory of the Homogeneous Nucleation of Ice from Supercooled Water, Thesis, The University of Chicago, (1967).

VITA

Richard Wayne Bolander was born March 26, 1940, at Parsons, Kansas. He attended the public schools in Lebanon, Missouri, and in Parsons, Kansas, graduating from Parsons Senior High School in 1957. From 1957 to 1961, he attended the University of Missouri School of Mines and Metallurgy, Rolla, Missouri, and received the Bachelor of Science Degree with a major in physics and minors in mathematics and electrical engineering. In 1961, he entered Texas Christian University and completed the requirements for the Master of Science Degree in physics in January, 1963. A teaching career was begun in 1963 as an Instructor in the Departments of Chemistry and Physics at Texas Woman's University, Denton, Texas. During the 1965-66 academic year, he served as an Assistant Professor of Physics at Louisiana Polytechnic Institute, Ruston, Louisiana. Since 1966, he has been enrolled in the Graduate School, University of Missouri - Rolla, as a candidate for the Doctor of Philosophy Degree in Physics. Three summers were spent in government and industrial research centers. Two summers were spent at the U. S. Naval Ordnance Laboratory, Silver Spring, Maryland, and one summer with General Dynamics Corporation / Fort Worth Division, Fort Worth, Texas.

Mr. Bolander is married to the former Barbara Meriwether. They have four children, William, Deborah, Thomas, and Robert.